bioRxiv preprint doi: https://doi.org/10.1101/118034; this version posted March 18, 2017. The copyright holder for this preprint (which was not certified by peer review) is the author/funder, who has granted bioRxiv a license to display the preprint in perpetuity. It is made available under aCC-BY 4.0 International license.

Identification, Isolation, and Characterization of Human LGR5-positive Colon Adenoma Cells

Michael K. Dame[1*], Durga Attili[1*], Shannon D. McClintock[1], Priya H. Dedhia[2], Peter Ouillette[1], Olaf Hardt[3], Alana M Chin[4], Xiang Xue[5], Julie Laliberte[6], Erica L Katz[1], Gina M Newsome[1], David Hill[7], Alyssa Miller[7,8], David Agorku[3], Christopher H Altheim[7], Andreas Bosio[3], Becky Simon[9], Linda C Samuelson[5,7], Jay A Stoerker[6], Henry D Appelman[1], James Varani[1], Max S. Wicha[9], Dean E. Brenner[9,10], Yatrik M. Shah[5,7], Jason R Spence[4,7], Justin A. Colacino[11,12]

Author contributions: Conceptualization: MD, DA, SM, JC, JS, YS, XX, JS, BS; Methodology: MD, DA, SM, OH, PO, DAg, AB; Investigation: MD, DA, SM, PD, PO, AC, XX, JL, EK, GN, DH, AM, DAg, CA; Analysis: JC, JS, HA, JL, PO; Resources: LS, OH, JS, CA; Original Draft: JC, MD, DA; Review-Editing: JS, YS, DB, LS, MW, JV; Supervision JC, JS, YS, DB, MW, JV

[1]Department of Pathology, University of Michigan Medical School, Ann Arbor, Michigan

[2]Department of Surgery, University of Michigan, Ann Arbor, Michigan

[3]Miltenyi Biotec GmbH, Bergisch Gladbach, Germany

[4]Department of Cell and Developmental Biology, University of Michigan, Ann Arbor, Michigan

[5]Department of Molecular and Integrative Physiology, University of Michigan, Ann Arbor, Michigan

[6]Progenity, Inc., Ann Arbor, Michigan

[7]Department of Internal Medicine, Division of Gastroenterology, University of Michigan Medical School, Ann Arbor, Michigan

[8]Cellular and Molecular Biology Program, University of Michigan, Ann Arbor, Michigan

[9]Department of Internal Medicine, Comprehensive Cancer Center, University of Michigan Medical School, Ann Arbor, Michigan

[10]Department of Pharmacology, University of Michigan, Ann Arbor, Michigan

[11]Department of Environmental Health Sciences, University of Michigan School of Public Health, Ann Arbor, Michigan

[12]Department of Nutritional Sciences, University of Michigan School of Public Health, Ann Arbor, Michigan

*- These authors contributed equally to this work

Short title: Isolation of human LGR5(+) colon adenoma cells

Correspondence: Justin Colacino, PhD
Department of Environmental Health Sciences
6651 SPH1, 1415 Washington Heights
Ann Arbor, MI, USA 48109
Email: colacino@umich.edu
Tel: 734-647-4347

bioRxiv preprint doi: https://doi.org/10.1101/118034; this version posted March 18, 2017. The copyright holder for this preprint (which was not certified by peer review) is the author/funder, who has granted bioRxiv a license to display the preprint in perpetuity. It is made available under aCC-BY 4.0 International license.

Abbreviations: DKK4, dickkopf WNT signaling pathway inhibitor 4; FGF20, fibroblast growth factor 20; FFPE, formalin fixed paraffin embedded; ISC, intestinal stem cell; ISH, *in situ* hybridization; LGR5, leucine-rich repeat-containing g-protein coupled receptor 5; MACS, magnetic-activated cell sorting; OLFM4, olfactomedin 4; TCGA, The Cancer Genome Atlas

Acknowledgments: We thank Kelly D. Maynard, Veda Yadagiri, Bodrul Islam, Kevin Kim, and Jessica Zhang for their support of the GISPORE Organoid Core facility; Missy Tuck, Brian Kleiner and Kim Gonzalez, clinical coordinators, the University of Michigan Hospitals, for their assistance in obtaining adenoma biopsies; Kristina Fields and Alan Burgess of the Research Histology and IHC Core; Dave Adams and Michael Dellheim of the UM BRCF Flow Cytometry Core; Deborah Postiff and Jackline Barikdar of the Tissue Procurement Core; Jeanne Geskes, Robert Lyons, and Melissa Coon, University of Michigan DNA Sequencing Core Facility; Ashwini Bhasi of the University of Michigan Bioinformatics Core; Robin Kunkel for graphic design, Department of Pathology; and Kaycee White and Muhammad N Aslam of the Histomorphometry Core, Department of Pathology, for their ScanScope service.

Funding: This study was supported by University of Michigan Comprehensive Cancer Center (M.S.W.) and UMCCC Fund for Discovery Pilot Project Award (J.A.C.) P30CA046592; MCubed (J.A.C.), a seed funding program at the University of Michigan; NIDDK 5P30DK034933 [The University of Michigan Center for Gastrointestinal Research (UMCGR)] and NIH NIAID U19AI116482 (J.R.S.); NCI CA148828 (Y.M.S.); NIH 5R01GM068848 and NIH P50CA130810 (GI SPORE, D.E.B., PI), the Kutsche Family Endowed Chair in the Department of Internal Medicine and the Geriatrics Research Education and Clinical Center at the Ann Arbor VA Medical Center (D.E.B.); NCI 3P30CA046592-26-S3 (M.S.W.); NIH R21 CA181855-01/02/03A1 and NCI R21CA201782-01(J.V.); American College of Surgeons, T32HD007505 (P.H.D.); X.X. was supported by the Research Scholar Award from American Gastroenterological Association; and A.M. was supported by the NIH Cellular and Molecular Biology Training Grant T32GM007315; the University of Washington Laboratory of Developmental Biology was supported by NIH 5R24HD000836 (Ian Glass, PI) from the Eunice Kennedy Shriver National Institute of Child Health & Human Development.

Disclosures: Olaf Hardt, David Agorku, and Andreas Bosio are full-time employees of Miltenyi Biotec GmbH. Julie Laliberte and Jay Stoerker are full-time employees of Progenity, Inc. The remaining co-authors declare that the research was conducted in the absence of any commercial or financial relationships that could be construed as a potential conflict of interest.

bioRxiv preprint doi: https://doi.org/10.1101/118034; this version posted March 18, 2017. The copyright holder for this preprint (which was not certified by peer review) is the author/funder, who has granted bioRxiv a license to display the preprint in perpetuity. It is made available under aCC-BY 4.0 International license.

ABSTRACT

The intestine is maintained by stem cells, marked by LGR5 expression, located at the base of crypts. Genetically engineered mouse models have provided information about marker genes and stem cell pathways. Less is known about human intestinal stem cells due to difficulty detecting and isolating these cells. We established an organoid repository from patient-derived adenomas, adenocarcinomas, and normal colon, which we analyzed for variants in 71 colorectal cancer (CRC) associated genes. Normal and neoplastic colon tissue organoids were analyzed for LGR5 expression by immunohistochemistry. LGR5-positive cells were isolated from 4 adenoma organoid lines and analyzed by RNA-sequencing. LGR5 expression in epithelium and stroma was associated with tumor stage. Integrating functional experiments with RNA-seq data from LGR5-positive adenoma organoid cells and normal colon, we associated expression of CRC-specific genes, including *DKK4*, with LGR5 expression. This system can be used to study LGR5-expressing cells in human tissue homeostasis and carcinogenesis.

Key words: biobank, organoid, stem cell, stroma, DKK4, enteroid, OLFM4, Wnt signaling, differentiation, regeneration, development

bioRxiv preprint doi: https://doi.org/10.1101/118034; this version posted March 18, 2017. The copyright holder for this preprint (which was not certified by peer review) is the author/funder, who has granted bioRxiv a license to display the preprint in perpetuity. It is made available under aCC-BY 4.0 International license.

INTRODUCTION

In adult mammals, the intestine is a site of rapid cellular turnover, mediated by a population of intestinal stem cells (ISCs) that reside at the base of intestinal crypts (Barker, van de Wetering, and Clevers 2008). These stem cells are identified by expression of several genetic markers in the mouse (van der Flier et al. 2009, Montgomery et al. 2011, Powell et al. 2012, Yan et al. 2012). Among these, *Lgr5* (leucine-rich repeat-containing g-protein coupled receptor 5) is the best characterized, and genetically modified mice provide a robust toolbox for isolating and manipulating these ISCs (Barker et al. 2007, Snippert et al. 2010, Sato et al. 2009). The LGR family of proteins (LGR4, 5, 6) code for receptors of the secreted R-spondin proteins (Rspo1- 4). Together, Lgr/Rspo acts to potentiate Wnt pathway signaling (Carmon et al. 2012, de Lau et al. 2011). Lineage tracing experiments have demonstrated that differentiated cell lineages in mouse small intestine and colonic crypts are clonally derived from *Lgr5*(+) ISCs (Barker et al. 2007). Additionally, lineage tracing studies have revealed that Lgr5 marks a population of stem-like cells within precancerous adenoma tissue that drive adenoma growth (Schepers et al. 2012), and human colorectal cancers overexpress *LGR5* (Junttila et al. 2015). Previous efforts to expand, isolate, and experimentally characterize primary human LGR5 cells have been hampered by two distinct issues: (1) The difficulty in obtaining cultures highly enriched for epithelial stem cells (Wang, Yamamoto, et al. 2015), and (2) a paucity of specific reagents to detect and isolate live LGR5(+) human cells (Barker 2014). To this effect, previous studies have reported varied localization of LGR5 within the normal crypt or did not assay normal tissue with antibody-based methods (Becker, Huang, and Mashimo 2008, Kleist et al. 2011, Fan et al. 2010, Takahashi et al. 2011, Kobayashi et al. 2012, Kemper et al. 2012). Recent efforts have utilized alternative strategies for the identification of LGR5(+) human colon cells, including *in situ* RNA hybridization (Jang, Lee, and Kim 2013, Baker et al. 2015). Due to these difficulties in the identification and isolation of human colon stem cells, the vast majority of knowledge about the role of LGR5(+) cells in colon tissue homeostasis and carcinogenesis is inferred from animal studies.

Intestinal organoid culture provides a method to culture tissue-derived cells that maintains the cellular heterogeneity in the intestinal epithelium (Sato, Stange, et al. 2011, Dedhia et al. 2016). Here we establish an

bioRxiv preprint doi: https://doi.org/10.1101/118034; this version posted March 18, 2017. The copyright holder for this preprint (which was not certified by peer review) is the author/funder, who has granted bioRxiv a license to display the preprint in perpetuity. It is made available under aCC-BY 4.0 International license.

organoid biobank of precancerous human adenoma tissues, as well as normal colon and colon adenocarcinoma. We report detailed and robust methods for the culture, identification, and isolation of human colon LGR5(+) cells from primary adenomas growing in long-term organoid culture using commercially available antibodies. Using these methods, we quantify LGR5 protein expression in human intestinal tissues, including a colon adenocarcinoma tissue microarray (TMA). Using magnetic bead and fluorescent activated cell sorting (FACS) to enrich and isolate LGR5(+) and LGR5(-) cells from organoids, we conducted RNA sequencing and defined the expression profile of human LGR5(+) adenoma cells. Here, we were able to make correlations between *LGR5* mRNA expression and the expression of *DKK4,* a gene not detectable in normal colon tissue but associated with colorectal cancer. We further extended the cell isolation methods to show they are robust, allowing for isolation of LGR5(+) cells from fresh normal human intestinal tissues. Collectively, we have identified novel associations between the ISC marker, LGR5, and cancer progression. Moreover, the methods and datasets presented provide powerful tools for basic biological studies of the role of LGR5(+) cells in human colon homeostasis, as well as translational studies in chemoprevention and precision medicine designed to target LGR5(+) cell populations.

MATERIALS AND METHODS

Establishment of organoid cultures from human colonic adenomas.

Isolation of human colonic crypts and adenomas; and culture and maintenance of adenoma organoid cultures, were performed using our previously described protocol (Dame et al. 2014). Adenoma tissue was acquired by endoscopy and adenocarcinoma tissue was collected from colonic resections according to protocols approved by the University of Michigan Institutional Review Board (IRB; HUM00064405/0038437/00030020). Normal colonic tissues were collected from deceased donors through the Gift of Life, Michigan (HUM00105750). De-identified human fetal intestinal tissue was obtained from the University of Washington Laboratory of Developmental Biology and approved by University of Michigan IRB (HUM00093465). Growth media used for organoid cultures included KGM-Gold™ (Lonza, Walkersville, MD; KGMG) (Dame et al. 2014), a serum-free epithelial medium containing epidermal growth factor (EGF) and pituitary extract; and L-WRN conditioned medium (Miyoshi and Stappenbeck 2013),

bioRxiv preprint doi: https://doi.org/10.1101/118034; this version posted March 18, 2017. The copyright holder for this preprint (which was not certified by peer review) is the author/funder, who has granted bioRxiv a license to display the preprint in perpetuity. It is made available under aCC-BY 4.0 International license.

containing high levels of Wnt3a, R-spondin-3 and Noggin, with added 10mM Nicotinamide (Sigma-Aldrich, St. Louis, Missouri). To drive organoids from a budding to cyst morphology, cultures were switched from the reduced medium, KGMG, to the stem cell support medium, L-WRN, for 3-4 weeks. Consistent with previous reports, organoids formed cystic structures in the presence of Wnt ligand provided by L-WRN medium (Sato, van Es, et al. 2011, Farin, Van Es, and Clevers 2012, Matano et al. 2015, Drost et al. 2015, Onuma et al. 2013). Cultures were propagated in Matrigel (Corning; Bedford, MA) which was made to 8mg/mL in growth media, in 6-well tissue culture plates. Cultures were passaged every 4-7 days by digesting Matrigel in cold 2mM EDTA and plated on the first day with 10µM Y27632 (Miltenyi Biotec; Bergisch Gladbach, Germany), a Rho-associated protein kinase (ROCK) inhibitor.

Single Cell Isolation and Magnetic separation for LGR5(+) and LGR5(-) cells

Single cell suspensions of adenoma organoids or normal intact colon tissue were generated using the Tumor Dissociation Kit (human; Miltenyi Biotec) in combination with the gentleMACS Dissociator (Miltenyi Biotec) with protocol modifications. The enzymes were prepared in HBSS modified to 0.13mM calcium and 0.9mM magnesium (10% standard HBSS concentrations) to minimize differentiation of the epithelial cells while supporting enzymatic activity. All plasticware, including cell strainers and columns, were 0.1% BSA-coated, and buffers contained 5-10µM Y27632. Cells were labeled with anti-LGR5 MicroBeads (human; Miltenyi Biotec) and the LGR5(+) cells were enriched by Magnetic-Activated Cell Sorting (MACS). Cells were applied through a cold BSA-coated 20µm cell strainer (CellTrics of Sysmex Europe GmbH; Norderstedt, Germany) to LS Columns (Miltenyi Biotec) in the above HBSS buffer containing 200 Kunitz units/mL DNAse (Sigma-Aldrich), 0.5% BSA in DPBS (Sigma-Aldrich), and 5µM Y27632. The magnet-bound positive and flow-through negative fractions were analyzed and isolated by FACS.

LGR5 Immunohistochemistry

Formalin fixed, paraffin sections were cut at 5-6 microns and rehydrated to water. Heat induced epitope retrieval was performed with FLEX TRS High pH Retrieval buffer (pH 9.01; Agilent Technologies,

bioRxiv preprint doi: https://doi.org/10.1101/118034; this version posted March 18, 2017. The copyright holder for this preprint (which was not certified by peer review) is the author/funder, who has granted bioRxiv a license to display the preprint in perpetuity. It is made available under aCC-BY 4.0 International license.

154 #K8004; Santa Clara, CA) for 20 minutes (Figure 1A, C and Figure 3A). After peroxidase blocking, the antibody LGR5 rabbit monoclonal clone STE-1-89-11.5 (Miltenyi Biotec, #130-104-945) was applied at a dilution of 1:50 (Figure 1A, C) or 1:100 (Figure 3A) at room temperature for 60 minutes. The FLEX HRP EnVision System (Agilent Technologies) was used for detection with a 10 minute DAB chromagen application. Note, sections freshly cut were compared to those that were stored at room temperature for 4 weeks, and showed more robust LGR5 staining (data not shown). The colon cancer tissue microarray (Figure 3A; 2 normal, 3 adenoma, 70 adenocarcinoma; 2 core samples per specimen) was freshly cut and provided by BioChain Institute, Inc. (Newark, CA; Z7020032, lot B508131).

LGR5 Immunohistochemistry scoring for staining intensity in the epithelium and in the stroma

The TMA, along with five additional FFPE normal colon samples from warm cadaveric colon resections, were scored for staining intensity in both the epithelium and then separately in the stroma (Figure 3). Scoring was conducted by two independent viewers on blinded samples at 8X and 20X magnification. Scoring key: 0 = non-specific or < 1%; 1 = 1-10% or only evident at 20X magnification; 2 = 10-50% or light diffuse staining >50%; 3 = >50%. Stage T2 (n=25) and T3 (n=44) tumors were compared to normal colon and adenoma (termed Stage T0; n=10). TMA cancers with grades I & I-II were grouped, termed “Grade I”, and cancers grade II-III & III were grouped, termed “Grade III” for further analyses. LGR5 stromal and epithelial staining for adenomas (n=3), cancer Grade I (n=20), II (n=38), and III (n=10) were compared to normal colon tissue (n=7).

Statistical Analyses

For IHC analyses, LGR5 stromal or epithelial staining intensity categories were plotted by tumor stage and grade using boxplots. Differences in LGR5 staining in the stroma or epithelium by stage or grade were quantified by linear regression, treating epithelial or stroma staining intensity (0, 1, 2, or 3) as a continuous dependent variable and either tumor stage or grade as a categorical independent variable, setting normal tissue as the reference group. For qPCR analyses, differences between biological replicates across experimental conditions were assessed using t-test. For both IHC and qPCR analyses, differences were

bioRxiv preprint doi: https://doi.org/10.1101/118034; this version posted March 18, 2017. The copyright holder for this preprint (which was not certified by peer review) is the author/funder, who has granted bioRxiv a license to display the preprint in perpetuity. It is made available under aCC-BY 4.0 International license.

considered statistically significant at $p < 0.05$. Statistical methodology for genomic variant characterization and RNA-sequencing differential expression analyses can be found in the Supplemental Information.

Detailed methods for organoid culture, genomic variant characterization, histological procedures and scoring, ISH, western analysis, LGR5(+) cell isolation and culture, flow cytometry, DKK4 analysis, RNA sequencing, and data analysis are provided in the Supplemental Information. All authors had access to the study data and reviewed and approved the final manuscript.

Data Access: The RNA-seq and genomic variant raw data are publically available at ArrayExpress under accession number E-MTAB-4698.

RESULTS

Isolation, Culture and genomic characterization of human adenoma organoids

We have developed an ongoing repository (Table 1) of organoids from patient-derived adenomas (n=17; including 2 high-risk sessile serrated adenomas), adenocarcinomas (n=4; including 1 colitis-associated cancer), and normal colon (n=9). All have been cryopreserved at early passage, reestablished from frozen stock, are mycoplasma-free, and have demonstrated long-term culture (i.e., > 6 months in continuous culture). The neoplasm-derived organoids have been genomically characterized for variants in a panel of common CRC driver mutations across 71 genes (Table 1).

LGR5 immunochemical specificity in human colon and intestine.

Two antibody clones for human LGR5 were used in this study: a rabbit monoclonal antibody generated against a peptide sequence of LGR5 (clone STE-1-89-11.5) and a rat monoclonal antibody generated to a full-length LGR5 protein (clone 22H2.8). At the onset of this study these antibodies were in development by Miltenyi Biotec, but now both antibodies are commercially available (Miltenyi Biotec GmbH, Bergisch Gladbach, Germany; see Methods and Supplemental Methods). Details of their development have been presented previously (Agorku et al. 2014, 2013), including the use of human *LGR4* and *LGR6* stable transfectants to demonstrate lack of cross-reactivity with these close homologues.

bioRxiv preprint doi: https://doi.org/10.1101/118034; this version posted March 18, 2017. The copyright holder for this preprint (which was not certified by peer review) is the author/funder, who has granted bioRxiv a license to display the preprint in perpetuity. It is made available under aCC-BY 4.0 International license.

Neoplasm	ID	Gender & Age		Location	Variants Detected
Adenoma (45mm)	282	F	66	ascending	APC Ala759fs, APC Gln1429*, ATM Arg337His, ATM Lys926Glu, EP300 Pro1802Pro, MSH2 R909Q
Adenoma (10mm)	300	M	59	transverse	APC Ser985fs, APC Arg1450*, BRCA1 Leu954Leu, BRAF Thr599dup, APC E1317Q
Adenoma (60mm)	469	M	86	cecum, ascending	APC Gln1378*, APC Glu536*, TCF7L2 Ser35fs, KRAS Gly12Asp, KRAS Gly12Ser
Adenoma (≥10mm)	569	F	18	sigmoid	APC Ser1355fs, ATM Phe858Leu, ATM Pro1054Arg, KRAS Ala146Thr, KRAS Gly12Val.
Adenoma (15mm)	574	F	69	hepatic flexure, proximal transverse	APC Arg876*, APC Glu1464*
Adenoma (30mm)	575	M	73	ascending	APC Arg1450*, APC His864fs, DMD Lys34Asn, KRAS Gln61His
Adenoma (20mm)	584	M	61	ascending	APC Thr1556fs, KRAS Ala146Val, MET Arg988Cys, PMS2 Gly29Ala, TP53 Arg267Trp, EP300 Asp1579Asn
Adenoma (35mm)	590	F	58	ascending	BUB1B Arg550*, FLCN His429fs, MLH1 Lys443fs, MSH3 Lys381fs, PALB2 Met296fs, TCERG1 Arg889fs, CTNNA1 Met826Thr, CTNNB1 Ser45Phe, MAP2K4 Val127Ala, MLH3 Pro564Ser, PIK3R1 Arg188Cys
Adenoma (15mm)	726	M	51	ascending	APC Ser837*, APC Arg1450* and AXIN2 Phe791Cys
Adenoma (25mm)	735	M	72	ascending	APC Leu665*, APC Arg1450*, CTNNB1 Ala126Ser, KRAS Gly12Asp
Adenoma (20mm)	772	F	79	rectum	APC Arg216*, APC Glu225*, AKT1 Gly393Gly, PIK3R1 Ile82fs
Adenoma (associated with adenocarcinoma)	14881	M	46	rectum	TP53 Pro151Ser, KRAS Gly12Asp, APC Pro1443fs
Adenoma: FAP (2 mm)	236	F	26	ascending	APC Thr1556fs, APC Leu143fs, MLH3 E624Q
Adenoma: Lynch	610	F	59	ascending	MSH3 Lys383fs, POLE Pro441Leu, DMD Val2498Ala, APC Ser1321Ser,KRAS Gln61His, PIK3CA Glu545Lys, ERBB2 Tyr411Cys, CDH1 His121Tyr, BLM Asn515fs, ERBB2 Pro1207His, MLH3 Asn674fs, APC Arg976fs, FBXW7 Ser668fs, AXIN2 Gly665fs, APC Ser1465fs, TCERG1 Arg958fs, BRCA2 Val1852Ile, GPC6 Gly243Trp, BRCA2 Lys1691fs, BRCA2 Thr3033fs, MUTYH Pro65fs, TCF7L2 Lys485fs, SLC9A9 Ala268Val, ERBB2 Arg47His, MSH2 R909Q
Adenoma (2-5mm)	664	M	52	cecum	MSH6 A20V
Adenoma: Sessile serrated (20mm)	245	F	54	ascending	BRAF Val600Glu, WBSCR17 Ser432Ser
Adenoma: Sessile serrated (23mm)	708	F	76	cecum	BRAF Val600Glu, DCC Asn472fs
Adenocarcinoma	781	F	52	descending	PIK3CA Glu545Lys, TP53 Phe113delPhe, APC Arg232*
Adenocarcinoma	815	F	74	cecum	KRAS Gly12Asp, APC Glu1309*, APC Glu1379*, MLH3 Asp1131Gly, EGFR Val323Ile, AKT1 Thr197Thr
Adenocarcinoma	861	F	76	ascending	SMAD4 Arg361His, PMS2 Thr9Ser, BRAF Val600Glu, APC Thr1556fs, APC Leu749fs, SLC9A9 Ala445Thr, BRCA1 Ser1517Pro, CDC27 Ala15Thr, WBSCR17 Ala577Val, PIK3CA Asn345Lys, DMD Arg550His, SLC9A9 Ile397fs, PMS2 M622I
Adenocarcinoma: IBD-associated	21	M	57	ascending	APC Gly1312*, TP53 Gly266Arg, PIK3CA Glu726Lys, KRAS Ala146Thr, BRAF Gly469Ala, PIK3CA Arg38Cys
Normal colon	78, 80, 81, 83, 84, 85, 87, 88, 89				F (ages 29, 33, 45, 49, 52, 56, 62), M (ages 21, 55); ascending

Table 1. Repository of patient-derived colon adenoma and adenocarcinoma organoids. A targeted colorectal cancer DNA sequencing panel was used to determine the presence of variants for 71 different oncogenes and tumor suppressor genes often mutated in colorectal cancers. Stop codon (*); frame shift (SS).

bioRxiv preprint doi: https://doi.org/10.1101/118034; this version posted March 18, 2017. The copyright holder for this preprint (which was not certified by peer review) is the author/funder, who has granted bioRxiv a license to display the preprint in perpetuity. It is made available under aCC-BY 4.0 International license.

LGR5 immunohistochemical (IHC) expression was localized with clone STE-1-89-11.5 to the crypt base columnar (CBC) cells, with rare staining in the stromal *lamina propria* in normal formalin fixed paraffin embedded (FFPE) colon (Figure 1a[1]). At high magnification this staining pattern was shown to mark thin cells (Figure 1a[2]), consistent with the morphology of CBC cells. From the same patient, an adenoma, adjacent to adenocarcinoma, showed intensified staining at the dysplastic crypt bases (Figure 1a[3]) and sporadic focal staining throughout the more disorganized epithelial component. In contrast to the matched normal tissue, stromal staining was pronounced in the adenoma associated with cancerous tissue (Figure 1a[3]). Supportive *LGR5 in situ* hybridization (ISH) staining was observed in the normal CBC cells (Figure 1B top panel); in the dysplastic epithelium (Figure 1B, arrow-1) and in the associated stroma (arrow-2).

The human fetal small intestine has been shown to express high levels of *LGR5* mRNA relative to adult by RNA-sequencing (Finkbeiner et al. 2015). Consistent with this, robust and specific LGR5 protein staining by IHC and immunofluorescence (Figure 1C), in conjunction with *LGR5* ISH (Figure 1D), was observed in the proliferative zone of the 15-week fetal gut. In contrast, IHC and IF staining in adult duodenum (Figure 2A) showed weak punctate LGR5(+) staining in cells present between Paneth cells marked by DefensinA5 (DEFA5), consistent with published ISH and RNA-sequencing data (Finkbeiner et al. 2015).

Clone STE-1-89-11.5 was further demonstrated to be specific for human LGR5 by Western blotting. Mouse 1881 lymphoma cells that were previously transfected with human *LGR5* served as a positive control [1881(+); provided by Miltenyi Biotec]. Transfection stability was confirmed by mRNA expression analysis (Figure 2B). The antibody showed strong reactivity against the human LGR5 1881(+) cell line, as well as measurable activity against one adenoma organoid (specimen #14881) (Figure 2C).

bioRxiv preprint doi: https://doi.org/10.1101/118034; this version posted March 18, 2017. The copyright holder for this preprint (which was not certified by peer review) is the author/funder, who has granted bioRxiv a license to display the preprint in perpetuity. It is made available under aCC-BY 4.0 International license.

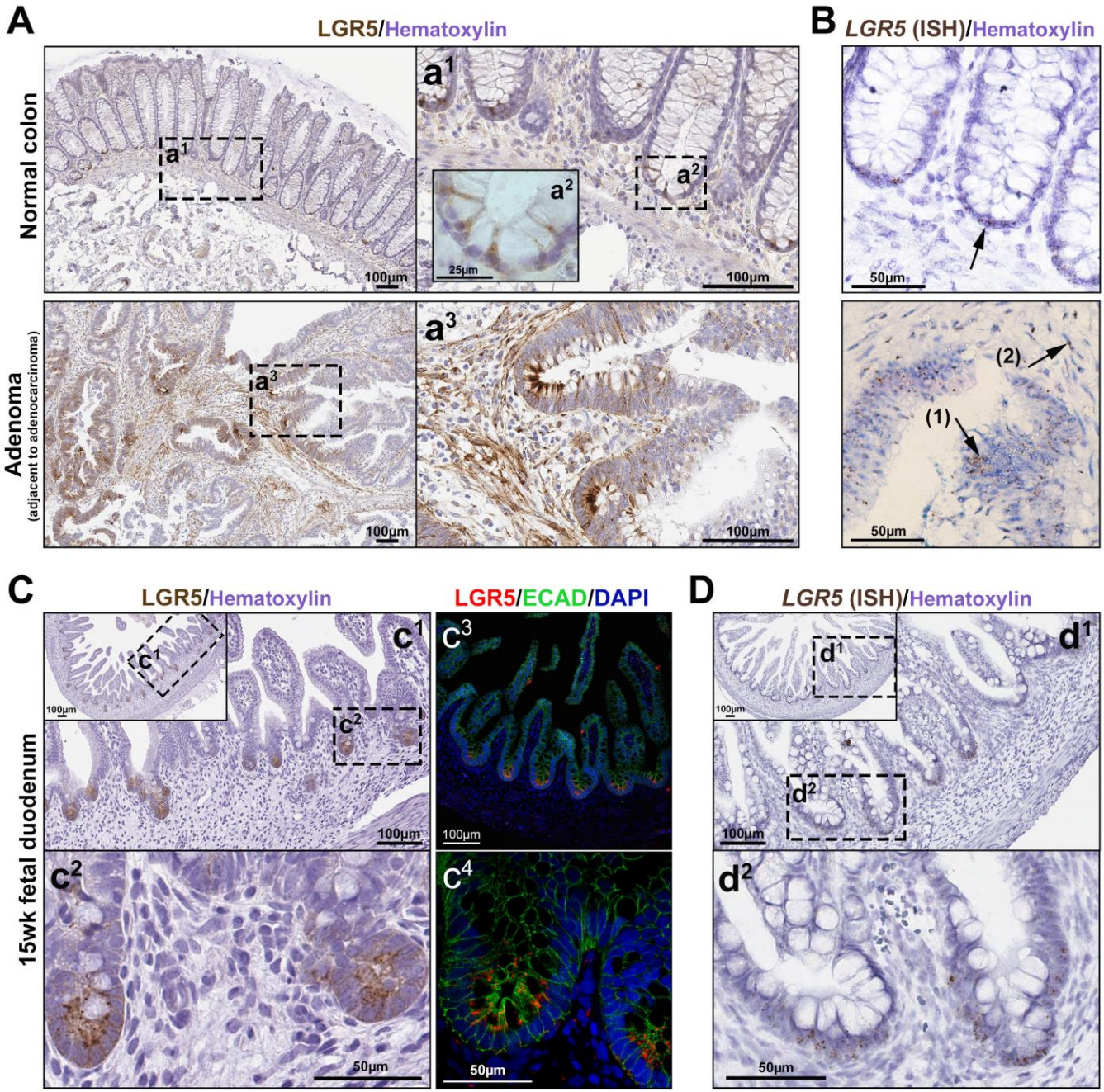

Figure 1. LGR5 immunochemical localization in human colon, colonic adenoma and duodenum.

(A) LGR5 IHC staining in normal human colon (one of five representative patients) at low (a1) and high (a2) magnification, as well as adenoma (high-grade dysplasia associated with an adenocarcinoma; specimen 14881) from the same patient (a3).

(B) LGR5 expression by in situ hybridization provides a conventional reference for the LGR5 staining in normal crypts (upper panel) and in the adenoma (bottom panel); glandular LGR5 (arrow-1) and stromal expression (arrow-2) in adenoma;

(C) LGR5 IHC (c1, c2) and IF staining (c3, c4) in fetal duodenum, and

(D) ISH expression in the same duodenum specimen.

bioRxiv preprint doi: https://doi.org/10.1101/118034; this version posted March 18, 2017. The copyright holder for this preprint (which was not certified by peer review) is the author/funder, who has granted bioRxiv a license to display the preprint in perpetuity. It is made available under aCC-BY 4.0 International license.

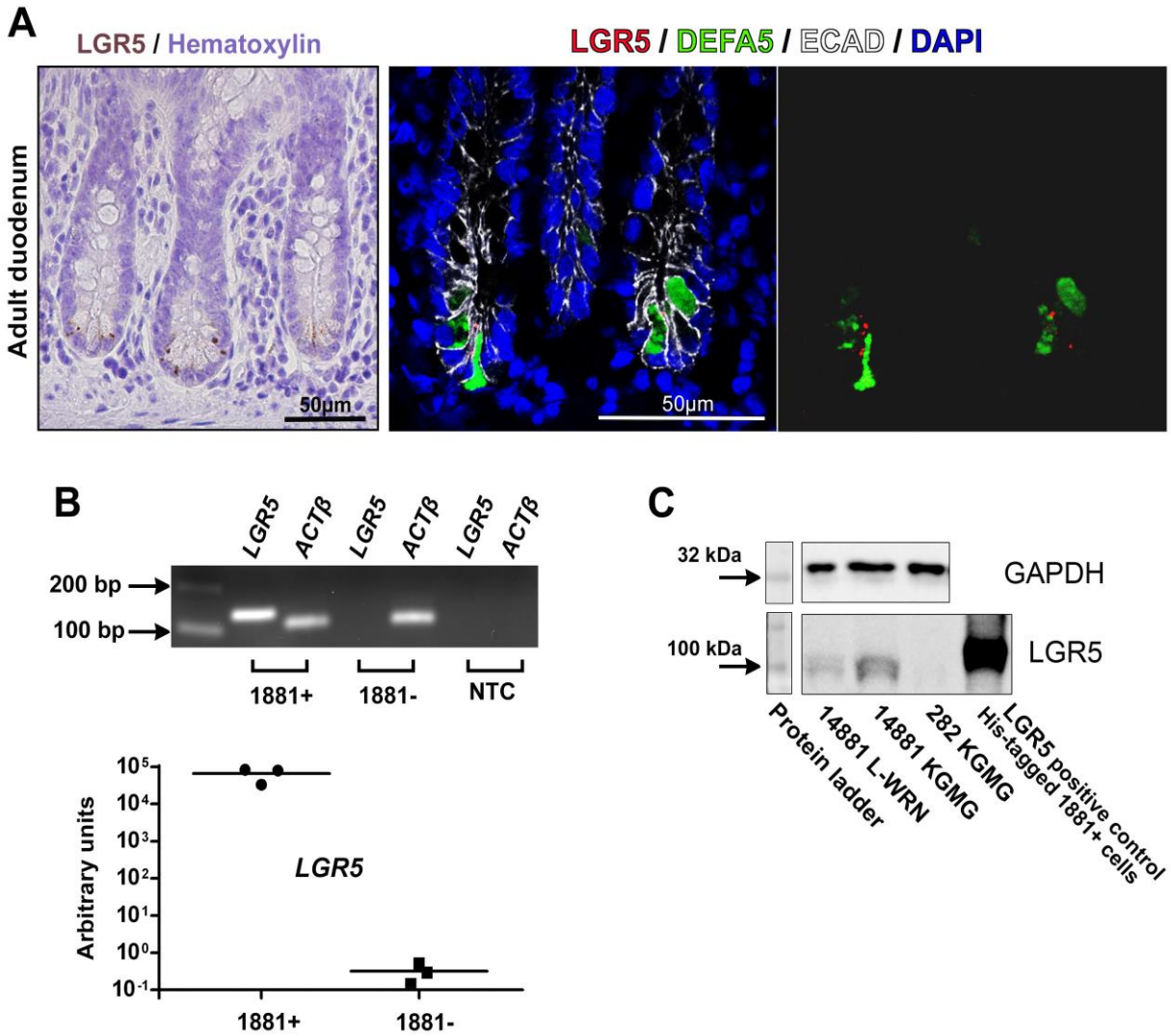

Figure 2. Further specificity analysis of human LGR5 antibody

(A) LGR5 immunohistochemical and immunofluorescent staining in adult duodenum showed weak punctate LGR5 expression, while adjacent cells stained with the paneth cell marker DefensinA5 (DEFA5) (middle and right panel).

(B) Mouse 1881 lymphoma cells were previously transfected with human *LGR5* [1881(+); Miltenyi Biotec]. To confirm transfection stability, the 1881 LGR5(+) and 1881 LGR5(-) cells were assayed for *LGR5* expression (n=3 biological replicates), and visualized with agarose gel analysis of qRT-PCR amplified products.

(C) Measurement of human LGR5 protein expression by Western blotting with the rabbit monoclonal anti-human LGR5 antibody clone STE-1-89-11.5 in 1881(+) cells, 282 adenoma organoids cultured in KGMG, and 14881 adenoma organoids cultured in KGMG or L-WRN.

bioRxiv preprint doi: https://doi.org/10.1101/118034; this version posted March 18, 2017. The copyright holder for this preprint (which was not certified by peer review) is the author/funder, who has granted bioRxiv a license to display the preprint in perpetuity. It is made available under aCC-BY 4.0 International license.

LGR5 *immunohistochemical expression in human colonic adenoma and adenocarcinoma; levels of glandular and stromal reactivity.*

LGR5 IHC staining was performed in a FFPE TMA, which included 2 normals, 3 adenoma, and 70 adenocarcinoma, with staining of 5 additional normal colon autopsy samples obtained for our studies (Figure 3). These were scored for staining intensity in the glandular epithelium and separately in the stroma. Unlike normal colon, which showed staining in select cells at the base of the crypt, the adenomas stained intensely in distinct zones of epithelium or for the entire dysplastic crypt (Figure 3A and Figure 4C, left column).

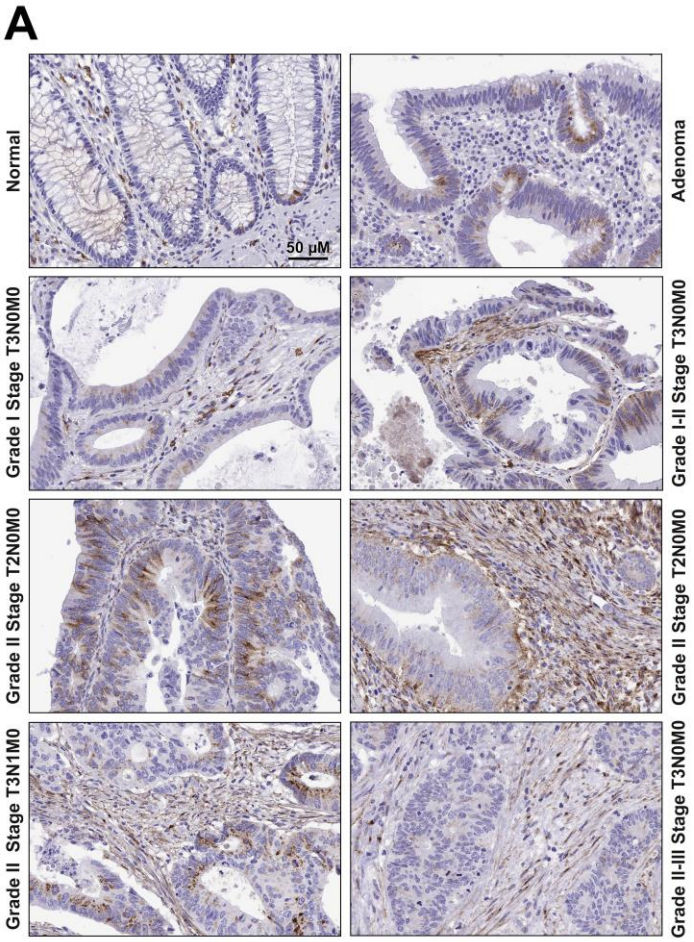

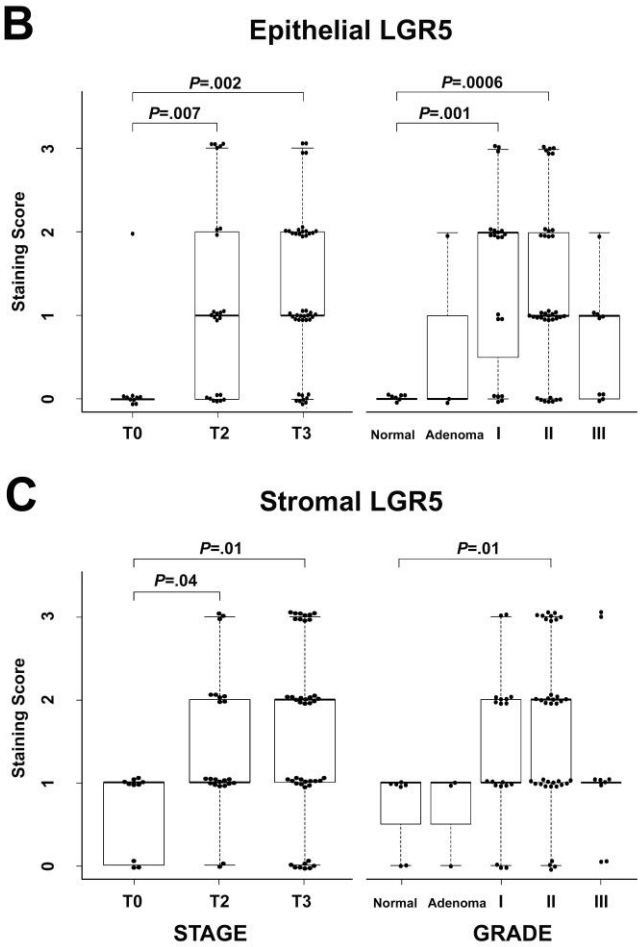

Figure 3. LGR5 immunohistochemical staining intensity in the epithelium and stroma across a range of colorectal adenocarcinoma stages and grades.

(A) Representative images of LGR5 staining in the epithelial and stromal components in normal colon (n=5 normal autopsy samples) and from a CRC tissue microarray (n=2 normals, 65-68 neoplasm).

(B) Association between epithelial or

(C) stromal staining intensity, and stage/grade of the tissue.

bioRxiv preprint doi: https://doi.org/10.1101/118034; this version posted March 18, 2017. The copyright holder for this preprint (which was not certified by peer review) is the author/funder, who has granted bioRxiv a license to display the preprint in perpetuity. It is made available under aCC-BY 4.0 International license.

Neoplastic tissue that retained crypt-like architecture, often showed pronounced LGR5 staining segregated to the base (Figure 1a[3]). Relative to normal tissue, the adenocarcinomas showed increased LGR5 staining in both the epithelium and in the stroma, with the greatest significance at higher cancer stages (Figure 3B, C; stage T3; epithelium P=.002; stroma P =.01) and grades (Grade II; epithelium P =.0006; stroma P =.01).

Strategy for the isolation of LGR5(+) cells from patient-derived adenoma organoids.

Figure 4A outlines the approach developed for isolation and analysis of LGR5(+) cells from human adenoma. Adenoma organoids were established in culture (approx. 2 months) and genomically characterized (Figure 4B lists mutations associated with individual specimens; see Table 1 for full organoid bank). The organoid cultures used in this study (14881, 282, 584, 590) were established in 'reduced medium', KGM-Gold™ (KGMG), a serum-free epithelial medium containing epidermal growth factor (EGF) and pituitary extract (Dame et al. 2014). When these organoid cultures were transferred to L-WRN medium (Miyoshi and Stappenbeck 2013) (which includes Wnt3a, R-spondin-3, Noggin, Nicotinamide, and EGF), they transitioned from budding structures (Figure 4C, middle column) to thin-walled spherical cysts (Figure 4C, right column), with the exception of organoid specimen 14881, which maintained a mix of thick-walled cysts and budding structures in L-WRN (not shown). Accompanying this shift in morphology was an increase in *LGR5* mRNA expression in L-WRN-cultured organoids compared to KGMG-cultured organoids, assessed by qRT-PCR (Figure 7A, left graph). Flow cytometric analysis revealed that L-WRN-cultured organoids had an increase in the number of LGR5 positive cells (Figure 4D, comparing "stain" in the first and second row; Figure S1). ImageStream analysis visually established the specificity of the fluorescently tagged LGR5 antibody to viable cells, rather than to cellular debris (Figure 4E). Even with L-WRN-enhanced LGR5, a low percentage of LGR5(+) cells was detected by flow cytometry, and therefore magnetic bead positive enrichment was used prior to FACS to increase the number of cells obtained.

bioRxiv preprint doi: https://doi.org/10.1101/118034; this version posted March 18, 2017. The copyright holder for this preprint (which was not certified by peer review) is the author/funder, who has granted bioRxiv a license to display the preprint in perpetuity. It is made available under aCC-BY 4.0 International license.

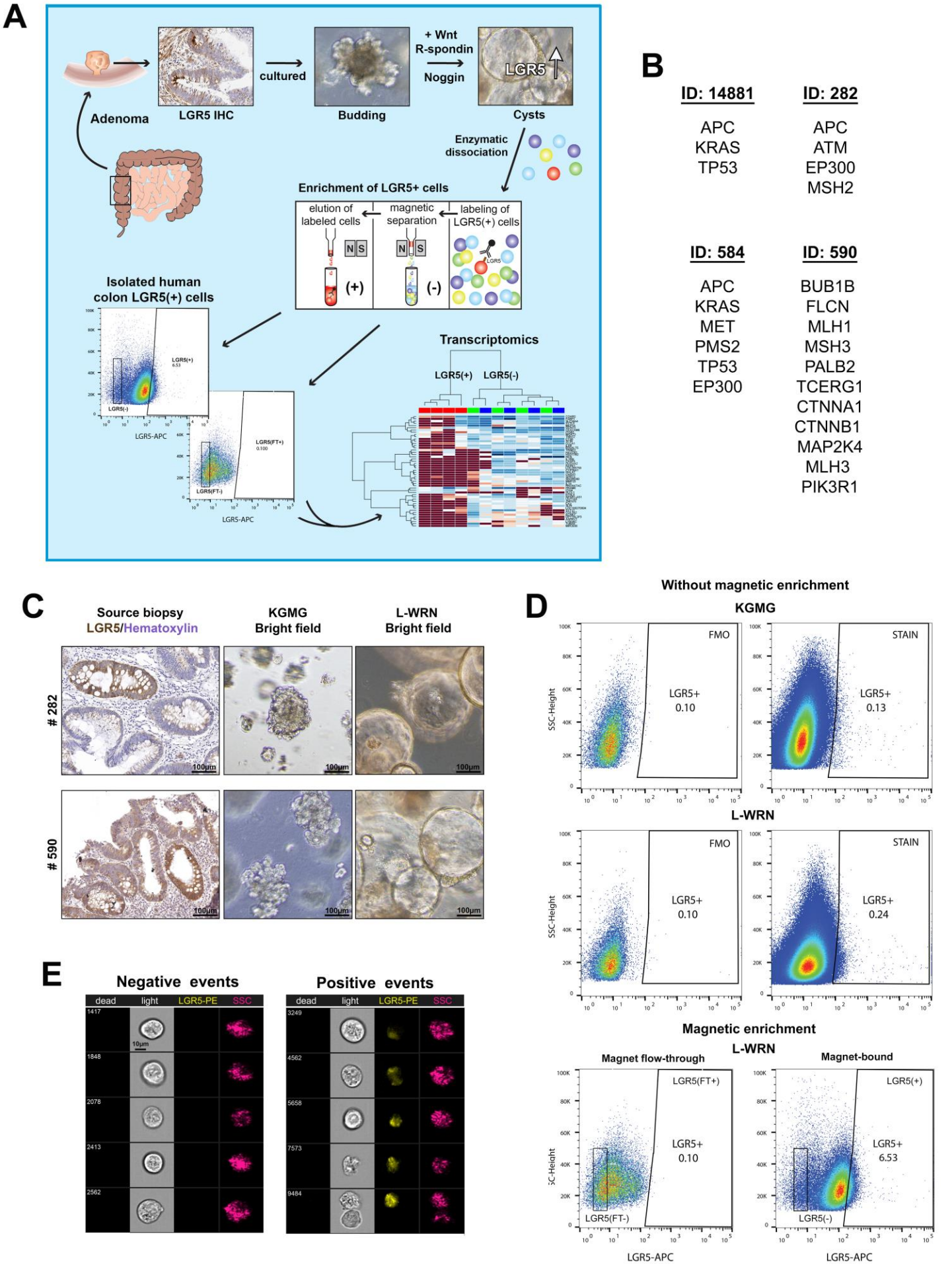

Figure 4

bioRxiv preprint doi: https://doi.org/10.1101/118034; this version posted March 18, 2017. The copyright holder for this preprint (which was not certified by peer review) is the author/funder, who has granted bioRxiv a license to display the preprint in perpetuity. It is made available under aCC-BY 4.0 International license.

Figure 4. **Strategy for the isolation of LGR5(+) cells from patient-derived colon adenoma.**

(A) Graphical representation of complete procedure.

(B) Establishment of an organoid culture repository from human colonic adenomas; genomic characterization of organoids (see Table 1 for full organoid bank).

(C) Culture of adenoma organoids for LGR5 enrichment. LGR5 IHC staining (left column) in biopsied large adenoma (> 10mm; two representative specimens are shown). Organoids with budding morphology (middle column) derived from these specimens cultured in the reduced medium KGMG. The same cultures with cystic morphology (right column) after being transferred for 3-4 weeks to L-WRN medium.

(D) Representative scatterplots of LGR5 expression in organoids cultured in KGMG or L-WRN (specimen 282). Live, LGR5(+) human adenoma cells were obtained after LGR5-magnetic bead enrichment by isolating DAPI(-) and LGR5(+) cellular populations.

(E) ImageStream analysis shows the cellular identity and positive antibody staining of sorted LGR5(+) events.

The 1881 LGR5(+) cells were used to validate the magnetic bead positive separation protocol and the high specificity of antibody clone 22H2.8. LGR5 expressing and non-expressing cells were mixed in varying proportions, magnetically separated, and analyzed by flow cytometry (Figure S1B). The initial ratio of 1881 LGR5(+) to 1881 LGR5(-) cells was predicted as shown by the pre-magnet flow histograms (Figure S1B, left column). The post-magnetic separation shows almost complete separation of 1881 LGR5(+) cells in the positive fraction (Figure S1B, right column) from 1881 LGR5(-) cells in the negative fraction (middle column).

After magnetic bead based enrichment of the adenoma organoid cells, the unbound flow-through negative population was used to set the LGR5 FACS gate (Figure 4D bottom row). Magnetic bead-bound LGR5(+) cells were isolated via FACS, and importantly, we observed that while only a small percentage of cells bound to beads were LGR5(+) (Figure 4D bottom row), on average, magnetic bead pulldowns of LGR5(+) cells led to an 9.2-fold enrichment in the number of LGR5(+) cells obtained compared to samples without magnetic enrichment, although this did vary with specimen (specimens 282, 584, 590; SE=6.8; n=4 sorts no magnet, n=8 sorts with magnet).

bioRxiv preprint doi: https://doi.org/10.1101/118034; this version posted March 18, 2017. The copyright holder for this preprint (which was not certified by peer review) is the author/funder, who has granted bioRxiv a license to display the preprint in perpetuity. It is made available under aCC-BY 4.0 International license.

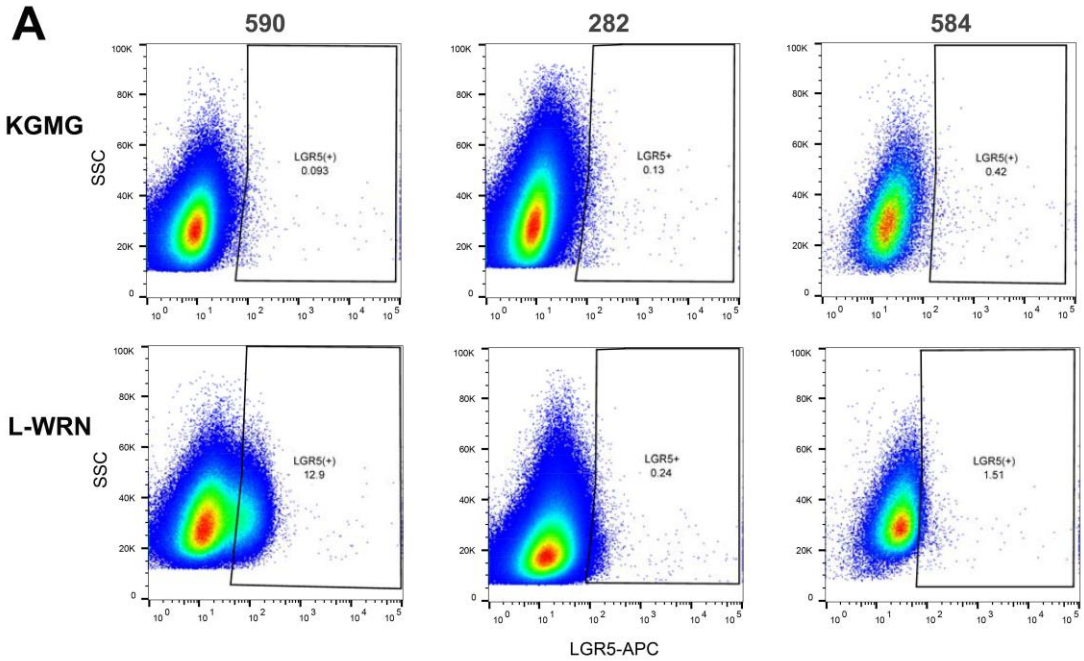

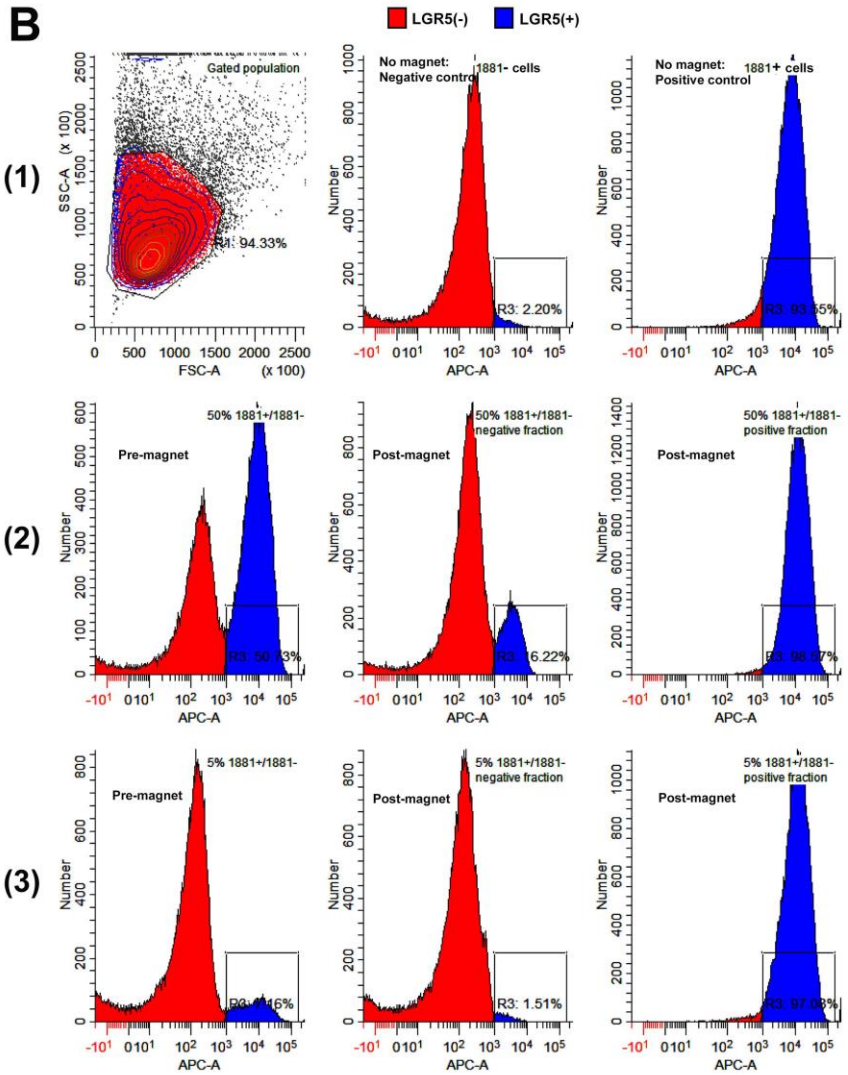

Figure S1 (related to Figure 4). Development of procedures for enrichment of LGR5(+) cells; L-WRN culture and magnetic-activated cell sorting (MACS).

(A) Flow cytometric analysis for enhanced number and fluorescent intensity of LGR5(+) cells resulting from organoids cultured in the reduced medium KGMG and then transferred for 3-4 weeks to L-WRN medium.

(B) Flow cytometry spike-in experiments to confirm LGR5 antibody specificity and to validate the magnetic bead enrichment strategy. (1) Pure populations of 1881 LGR5(+) and 1881 LGR5(-) cells were analyzed by flow to establish gating strategy. 1881 LGR5(+) and 1881 LGR5(-) cells were mixed in the proportions, (2) 50/50 and (3) 5/95; and analyzed by flow cytometry before (left column) and after magnetic separation (middle/right columns) with rat monoclonal anti-human LGR5 antibody clone 22H2.8.

bioRxiv preprint doi: https://doi.org/10.1101/118034; this version posted March 18, 2017. The copyright holder for this preprint (which was not certified by peer review) is the author/funder, who has granted bioRxiv a license to display the preprint in perpetuity. It is made available under aCC-BY 4.0 International license.

Transcriptomic profiling of LGR5(+) adenoma cells

The gene expression signature of human LGR5(+) intestinal cells is essentially uncharacterized, which has significantly limited our understanding of the role of these cells in human intestinal stem cell biology and colorectal cancer progression. Using the methods described above, we isolated LGR5(+) cells from four different adenoma-derived organoid lines and conducted RNA-seq on three sorted cellular populations from each (Figure 5, Figure S2): (1) magnetic column flow-through cells, termed LGR5(FT-); (2) cells bound to the magnet, but LGR5 negative based on FACS, termed LGR5(-); and (3) cells bound to the magnet and LGR5 positive based on FACS, termed LGR5(+). Genomic variant analysis showed that each of these patient specimens has functionally significant mutations within commonly mutated colon cancer genes, confirming the adenoma, and not normal, identity of these organoids grown in L-WRN (Table 1). Expression profiles of the LGR5(-) and LGR5(FT-) were found to be largely similar at both the gene expression and pathway level (Figure S2C, D). The transcriptome-wide similarity between these two LGR5-negative populations suggests that magnetic bead enrichment alone is not sufficient to isolate LGR5(+) cells. Due to transcriptional similarity between negative populations, our analysis focused on comparisons between the magnetic bead-bound cells deemed to be LGR5(+) and LGR5(-) by FACS (Figure 5).

Multidimensional scaling on the top 500 most variably expressed genes revealed that samples clustered distinctly by the patient of origin, not by the expression of LGR5 (Figure 5A, Figure S2A). Despite this, we identified 519 differentially expressed genes (FDR P-value < .05) between the two cell fractions across the four genetically diverse adenomas (Figure 5B and Table S1). Expression values for all differentially expressed genes for each specimen, as well comparisons between LGR5(+) cells and LGR5(FT-) cells, are reported in Table S1. We determined that *LGR5* had the highest level of statistical enrichment in the LGR5(+) cells (FDR=3.8E-21) and was expressed an average of 5.5 fold higher compared to LGR5(-) cells, lending confidence to the specificity of the LGR5 antibody and the separation procedure. Unsupervised hierarchical clustering analysis using the top 50 most differentially expressed genes showed clear separation between the LGR5(+) and LGR5(-) samples from three of the four enteroid lines (Figure 5C), suggesting both commonalities and heterogeneity in the LGR5(+) cell gene expression signature

bioRxiv preprint doi: https://doi.org/10.1101/118034; this version posted March 18, 2017. The copyright holder for this preprint (which was not certified by peer review) is the author/funder, who has granted bioRxiv a license to display the preprint in perpetuity. It is made available under aCC-BY 4.0 International license.

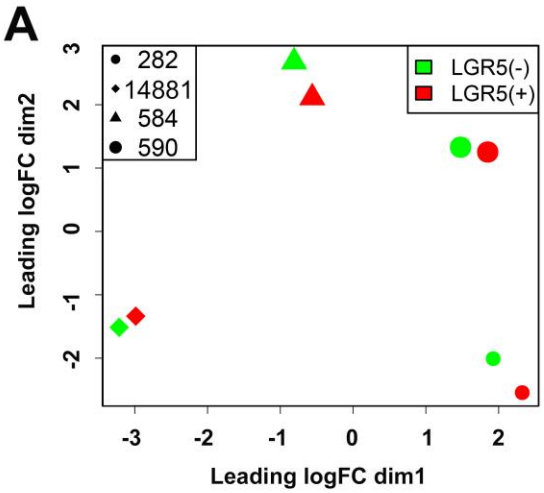

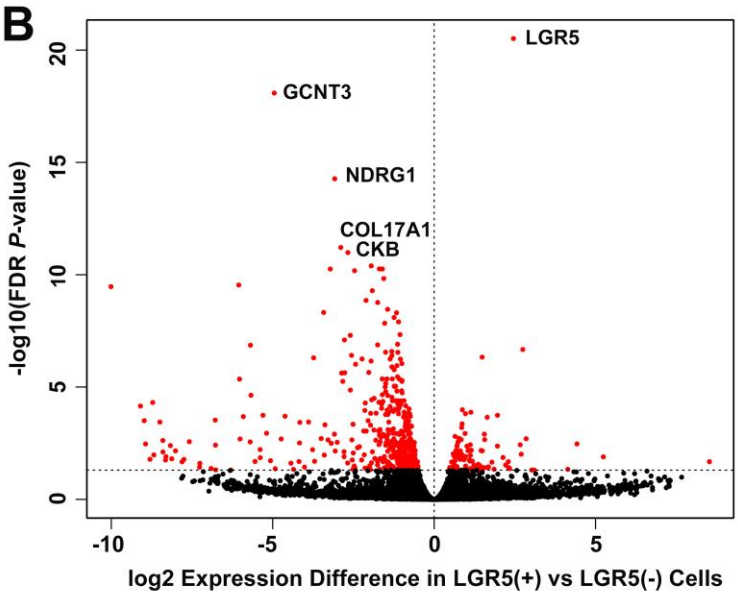

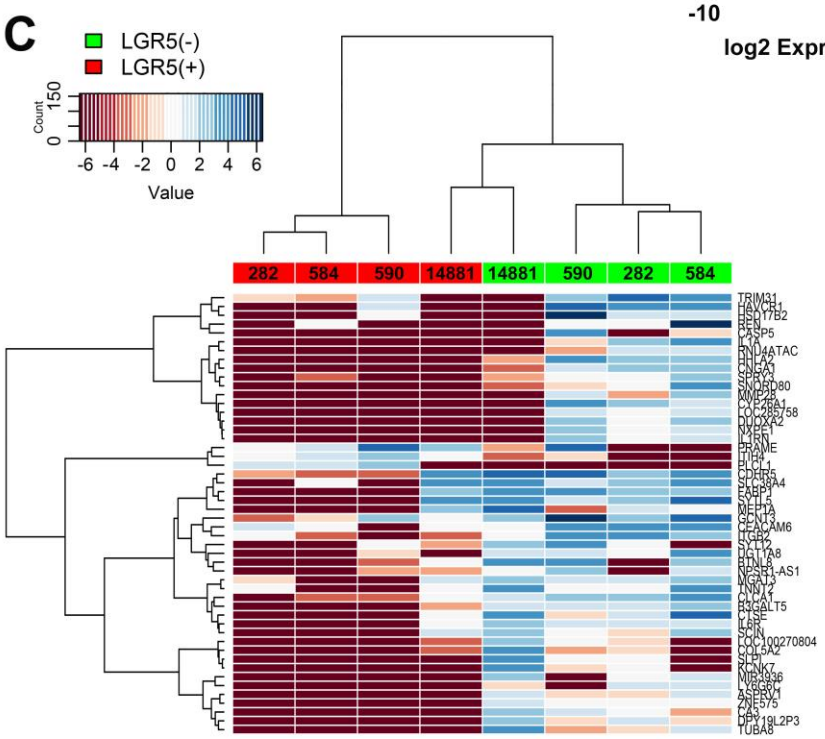

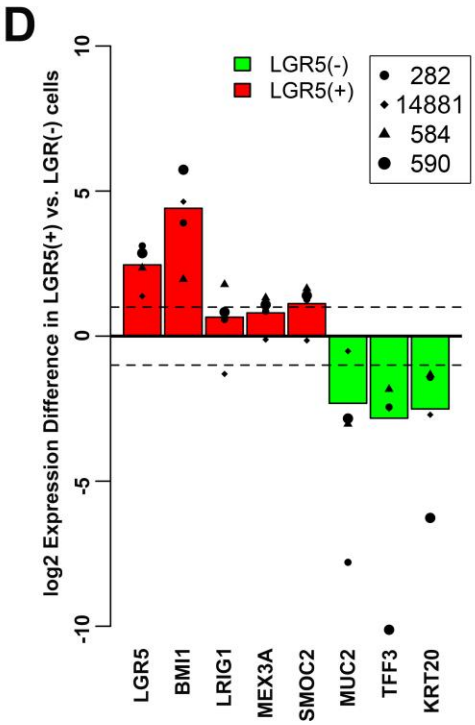

E

Pathway Name	LGR5(+) vs (-) Rank	& *P*-Value
Glycolysis / Gluconeogenesis	1	6.57E-09
Biosynthesis of amino acids	2	4.32E-07
Metabolic pathways	3	7.55E-06
HIF-1 signaling pathway	4	1.42E-05
Carbon metabolism	5	1.45E-05
Fructose and mannose metabolism	6	3.25E-04
Cytokine-cytokine receptor interaction	7	4.06E-04
Glycosphingolipid biosynthesis	8	4.42E-04
Central carbon metabolism in cancer	9	5.60E-04
Hematopoietic cell lineage	10	6.06E-04

Figure 5

bioRxiv preprint doi: https://doi.org/10.1101/118034; this version posted March 18, 2017. The copyright holder for this preprint (which was not certified by peer review) is the author/funder, who has granted bioRxiv a license to display the preprint in perpetuity. It is made available under aCC-BY 4.0 International license.

Figure 5. Transcriptomic profiling of human LGR5(+) and LGR5(-) primary adenoma cells isolated from four patient-derived organoid cultures.

(A) Multidimensional scaling plot of the LGR5(+) and LGR5(-) cells, based on the top 500 most variable genes. Patient identifiers #14881, 228, 584, and 590.

(B) False discovery rate (FDR) volcano plot of the log(2) ratio of gene expression between the LGR5(+) and LGR5(-) cells.

(C) Unsupervised hierarchical clustering heatmap of the 50 most differentially expressed genes by fold change between the LGR5(+) (red) and LGR5(-) (green) populations.

(D) Log(2) fold change in gene expression between LGR5(+) and LGR5(-) cells for known markers of colon stem (red) and differentiated (green) cells.

(E) The top 10 most enriched KEGG pathways for differentially expressed genes between the LGR5(+) and LGR5(-) cells.

Figure S2 (Related to Figure 5). Transcriptomic profiling of human LGR5(+) primary adenoma cells; comparisons between sorted MACS magnet-bound LGR5(-) and sorted MACS flow-through LGR5(FT-) cells.

(A) Multidimensional scaling plot of the LGR5(+), sorted MACS magnet-bound LGR5(-) cells, and sorted MACS flow-through LGR5(FT-) cells based on the top 500 most variable genes.

(B) Unsupervised hierarchical clustering heatmap of the 50 most variable genes between the LGR5(+) (red), LGR5(-) (green), and LGR5(FT-) (blue) populations.

(C) The top 10 most enriched KEGG pathways for differentially expressed genes between the LGR5(+) and LGR5(-); and LGR5(+) and LGR5(FT-) cells.

(D) Gene expression overlap between the [LGR5(+) vs. LGR5(-)], [LGR5(+) vs. LGR5(FT-)], and [LGR5(-) vs. LGR5(FT-)]

between specimens. When the expression signature of LGR5(+) cells were clustered with those from both the LGR5(-) and LGR5(FT-) cells, however, there was clear separation of the LGR5(+) cells across all four organoid lines (Figure S2B). Stem cell markers associated with the colon as well as other tissue-specific stem cells including *BMI1*, *MEX3A*, and *SMOC2* were upregulated in LGR5(+) cells, while known markers of colonic differentiation, including *MUC2*, *TFF3*, and *KRT20* were down-regulated (Figure 5D). Pathway analyses revealed differential expression in LGR5(+) cells for genes involved in metabolism, including the pathways, *glycolysis and gluconeogenesis*, *biosynthesis of amino acids*, *metabolic pathways*, *carbon metabolism*, *fructose/mannose metabolism*, *glycosphingolipid biosynthesis*, and *central carbon metabolism*

bioRxiv preprint doi: https://doi.org/10.1101/118034; this version posted March 18, 2017. The copyright holder for this preprint (which was not certified by peer review) is the author/funder, who has granted bioRxiv a license to display the preprint in perpetuity. It is made available under aCC-BY 4.0 International license.

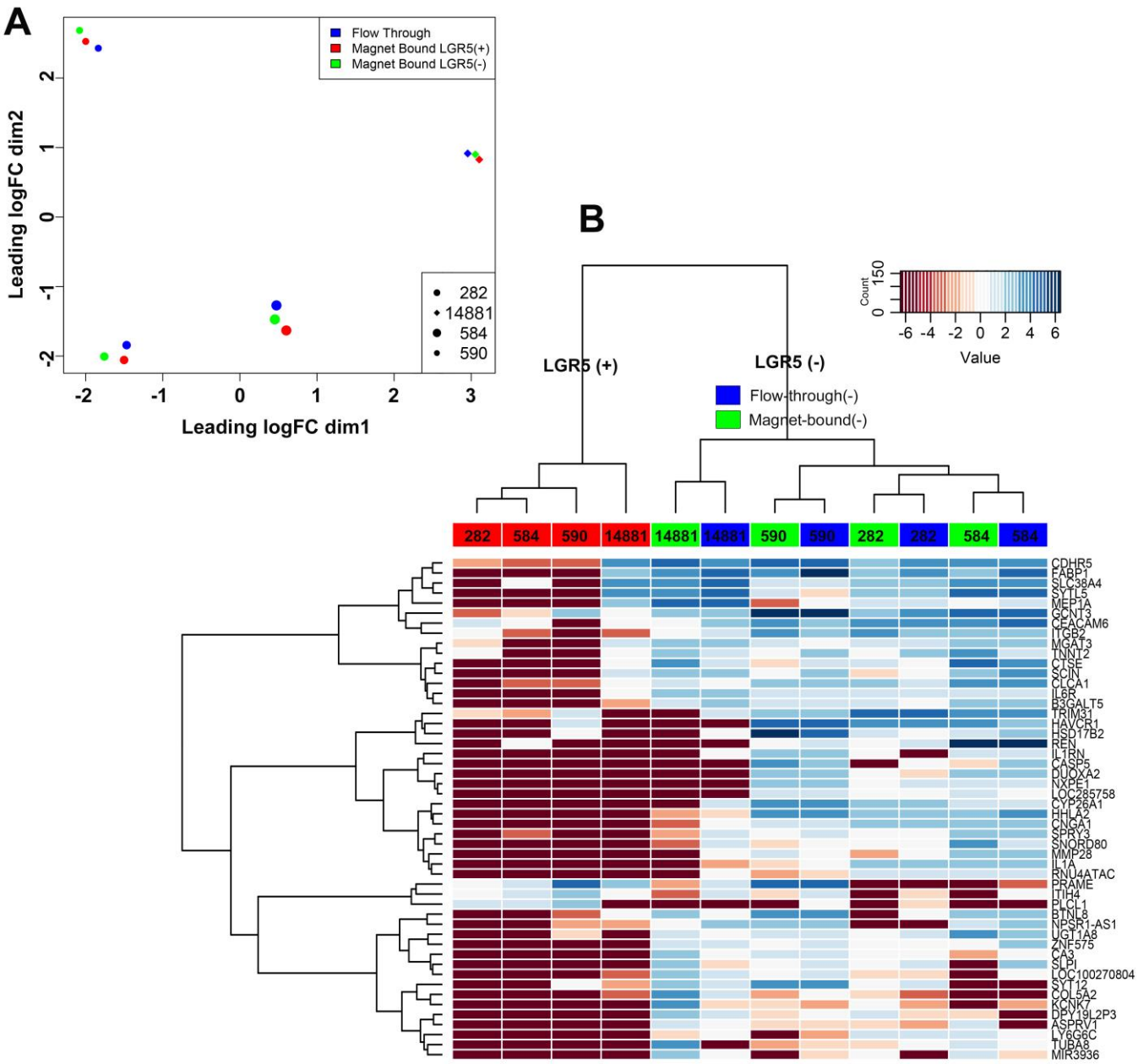

C

Pathway Name	LGR5(+) vs (-) Rank	LGR5(+) vs (-) *P*-Value	LGR5(+) vs FTN Rank	LGR5(+) vs FTN *P*-Value
Glycolysis / Gluconeogenesis	1	6.57E-09	1	1.06E-07
Biosynthesis of amino acids	2	4.32E-07	5	1.81E-04
Metabolic pathways	3	7.55E-06	3	1.40E-05
HIF-1 signaling pathway	4	1.42E-05	2	1.16E-05
Carbon metabolism	5	1.45E-05	13	5.52E-03
Fructose and mannose metabolism	6	3.25E-04	25	1.70E-02
Cytokine-cytokine receptor interaction	7	4.06E-04	4	6.21E-05
Glycosphingolipid biosynthesis	8	4.42E-04	6	5.37E-04
Central carbon metabolism in cancer	9	5.60E-04	20	1.26E-02
Hematopoietic cell lineage	10	6.06E-04	29	1.82E-02

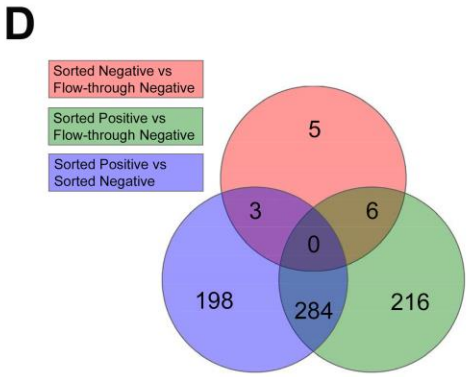

Figure S2

bioRxiv preprint doi: https://doi.org/10.1101/118034; this version posted March 18, 2017. The copyright holder for this preprint (which was not certified by peer review) is the author/funder, who has granted bioRxiv a license to display the preprint in perpetuity. It is made available under aCC-BY 4.0 International license.

in cancer (Figure 5E; Figure S2C). Additionally, LGR5(+) cells had significantly differentially expressed genes involved in *HIF-1 signaling*, *cytokine-cytokine receptor interaction*, *hematopoietic cell lineage*, *MAPK signaling*, *PI3K/AKT signaling*, and *pathways in cancer* (Table S1; Figure 5E, Figure S2C, Figure S3-8).

We also identified a high level of concordance between LGR5(+) cells and a previously reported set of genes associated with high levels of Wnt signaling in mouse cancer stem cells (based on TOP-GFP Wnt reporter activity (Vermeulen et al. 2010) (Figure 6A). In order to identify a "human adenoma LGR5(+) cell gene signature" with more stringent parameters, we compared genes upregulated in LGR5(+) cells to both LGR5(-) and to LGR5(FT-) cells to which we identified 33 genes (Table 2). A comparison between these 33 genes in the "human adenoma LGR5(+) cell gene signature" and the previously published "murine intestinal stem cell signature," generated from isolated Lgr5^{HI} ISCs (Munoz et al. 2012), identified 4 overlapping genes that were enriched in both populations, including the canonical ISC markers *LGR5*, *SMOC2*, and *CDCA7* (Figure 6B). This analysis also revealed a large number of genes in the human adenoma LGR5(+) cell signature that did not overlap with the mouse Lgr5 stem cell signature.

Gene	(+) vs. (-)		(+) vs. (FT-)	
	logFC	FDR	logFC	FDR
LGR5	2.456	3.1E-21	2.896	9.9E-30
PLA2G2A	2.746	2.1E-07	1.990	1.9E-04
STARD9	1.487	4.7E-07	0.942	0.005
STK38L	0.874	1.0E-04	0.669	0.008
TBC1D1	0.971	1.5E-04	1.044	4.0E-05
MYRIP	1.963	1.8E-04	1.801	0.001
ITPR2	0.866	4.4E-04	0.735	0.005
ZAK	0.854	0.001	0.785	0.002
INHBB	1.555	0.001	1.990	8.6E-06
APBB2	0.647	0.002	0.529	0.019
RHEB	0.770	0.002	0.613	0.027
PRSS56	1.566	0.002	2.242	8.0E-07
PTPRD	0.740	0.003	0.743	0.003
PRAME	4.424	0.003	3.403	0.028
SMOC2	1.121	0.004	1.329	2.9E-04
SLC39A6	0.709	0.004	0.643	0.013
MAP1A	1.152	0.006	1.182	0.005
HNRPDL	0.589	0.009	0.550	0.020
ICK	0.858	0.010	0.774	0.027
KREMEN1	0.740	0.013	0.936	0.001
SCRN1	0.932	0.017	0.880	0.027
TMEM19	1.097	0.018	1.047	0.028
ABCB1	0.645	0.019	0.701	0.008
TGFB3	1.181	0.020	1.274	0.009
ZNF219	1.106	0.020	1.113	0.021
GLT25D2	1.365	0.027	1.601	0.004
CTNNB1	0.632	0.030	0.798	0.002
GINS2	1.231	0.030	1.210	0.032
IL17RD	0.653	0.036	0.759	0.007
CDCA7	0.623	0.038	0.612	0.042
CFTR	0.484	0.038	0.493	0.031
LRP4	0.677	0.047	0.896	0.002
HIP1	0.852	0.049	0.870	0.039

Table 2. Genes upregulated in human adenoma LGR5(+) cells when compared to both LGR5(-) and to LGR5(FT-)

bioRxiv preprint doi: https://doi.org/10.1101/118034; this version posted March 18, 2017. The copyright holder for this preprint (which was not certified by peer review) is the author/funder, who has granted bioRxiv a license to display the preprint in perpetuity. It is made available under aCC-BY 4.0 International license.

Given that our transcriptional analysis compared cells, LGR5(+) vs. LGR5(-), isolated from adenoma-derived organoid cultures (as opposed to intact tissue biopsies), we reasoned that it was possible that LGR5(+) enriched genes might be masked by comparing fractions which in whole were cultured in medium that promotes high levels of WNT signaling (L-WRN). Therefore, we compared LGR5(+) cells with previously published RNA-seq data from whole-thickness normal human colon (Uhlen et al. 2015) (Figure 6C, D). When we compared the 33 genes from our "human adenoma LGR5(+) cell gene signature" (Table 2) to normal colon, we observed a strong enrichment for a majority of the genes (Figure 6C). In an unbiased comparison of all genes (Figure 6D), two of the most over-expressed genes by overall fold change in LGR5(+) adenoma cells compared to normal colon were the Wnt pathway inhibitor *DKK4* (dickkopf WNT signaling pathway inhibitor 4) and *FGF20* (fibroblast growth factor 20). Both were virtually undetectable in the normal colon (Table S1). An analysis of TCGA colorectal cancer gene expression data (The Cancer Genome Atlas 2012) revealed that both *DKK4* and *FGF20* are significantly upregulated in colorectal tumors compared to normal tissue (Figure 6E).

Figure 6. Comparisons between genes in the human adenoma LGR5(+) cell gene signature and previously published murine and human signatures.

(A) Concordance of adenoma LGR5(+) cell gene expression with gene expression associated with Wnt signaling in mouse cancer stem cells, based on TOP-GFP Wnt reporter activity (Vermeulen et al. 2010).

(B) Gene expression overlap between genes upregulated in LGR5(+) vs. LGR5(-) cells and the *Lgr5* mouse intestinal stem cell signature reported in Muñoz et al (Munoz et al. 2012).

(C) Comparison of gene expression between LGR5(+) adenoma cells and previously published RNA-seq data from normal human colon (Uhlen et al. 2015) for genes in the "human adenoma LGR5+ cell gene signature.

(D) The top ten most differentially expressed genes by magnitude between LGR5(+) adenoma cells and normal human colon (all genes; unbiased analysis) (Uhlen et al. 2015).

(E) An analysis of TCGA colorectal cancer gene expression data through Oncomine™ of DKK4 and FGF20 comparing colorectal adenocarcinoma expression with normal colon and rectum.

bioRxiv preprint doi: https://doi.org/10.1101/118034; this version posted March 18, 2017. The copyright holder for this preprint (which was not certified by peer review) is the author/funder, who has granted bioRxiv a license to display the preprint in perpetuity. It is made available under aCC-BY 4.0 International license.

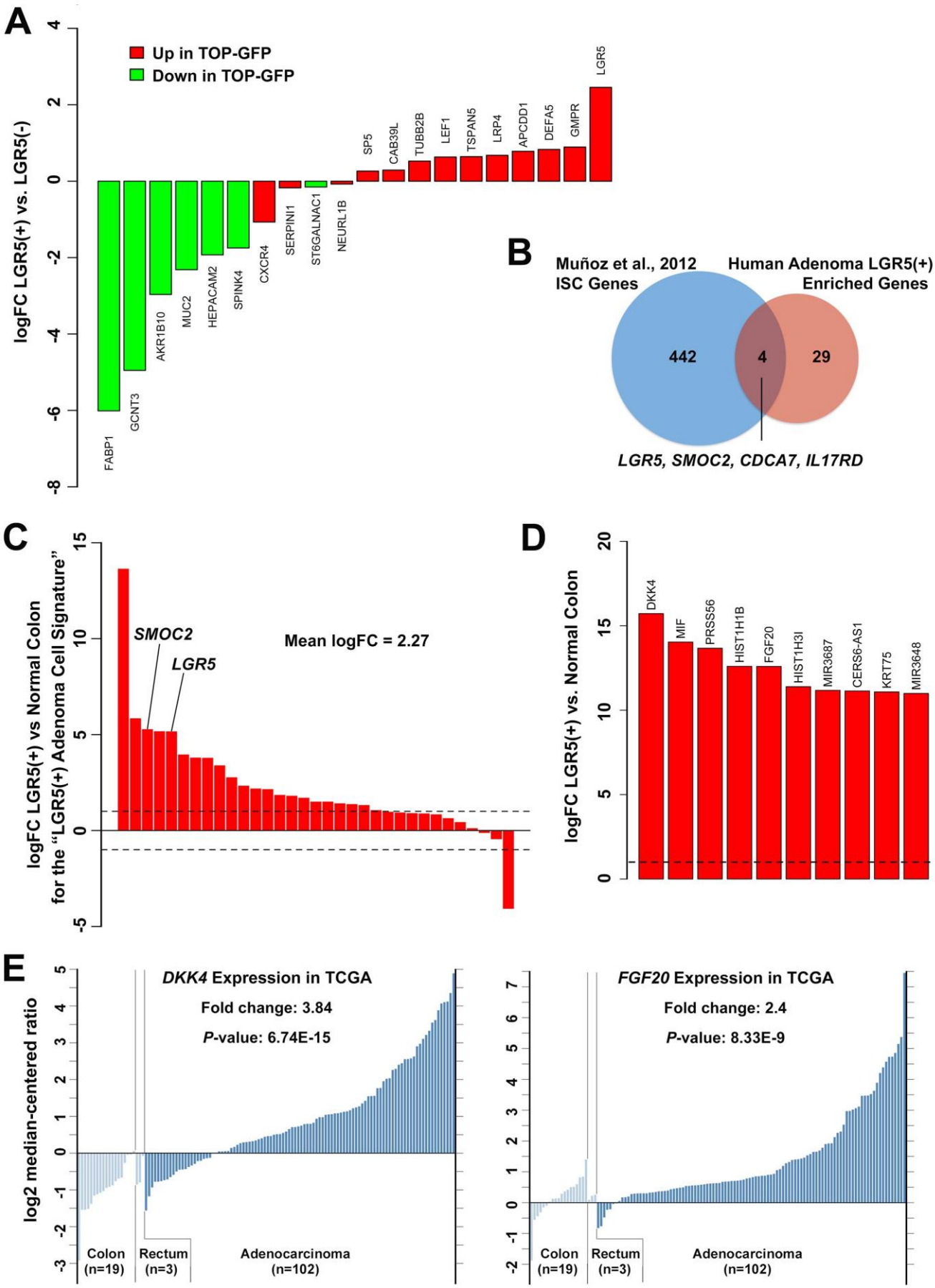

Figure 6

bioRxiv preprint doi: https://doi.org/10.1101/118034; this version posted March 18, 2017. The copyright holder for this preprint (which was not certified by peer review) is the author/funder, who has granted bioRxiv a license to display the preprint in perpetuity. It is made available under aCC-BY 4.0 International license.

We further assessed *DKK4* in 3 of the 4 of adenoma organoids (282, 584, 590) in which *DKK4* was expressed at higher levels in the LGR5(+), relative to LGR5(-) cells (4-fold, 1.9E-06 FDR; Table S1), by comparing expression when cultured in L-WRN vs KGMG. Both *LGR5* (average fold change 4.6±1.2SE) and *DKK*4 (average fold change 174.3±146SE) show significantly enhanced expression in organoids when cultured in L-WRN (Figure 7B). When these organoids were treated with recombinant human DKK4 for 72hrs, there was no significant change in *LGR5* expression in either KGMG or L-WRN (Figure 7C). With a *DKK4* stable organoid knockdown (specimen 282), LWRN-enhanced *DKK4* expression was significantly attenuated, but LWRN-enhanced *LGR5* expression did not change (Figure 7D). Taken together, these data suggest that DKK4 may not play a significant role in LGR5(+) stem cell maintenance, but that DKK4 could be a novel marker associated with LGR5 expression in neoplastic tissue.

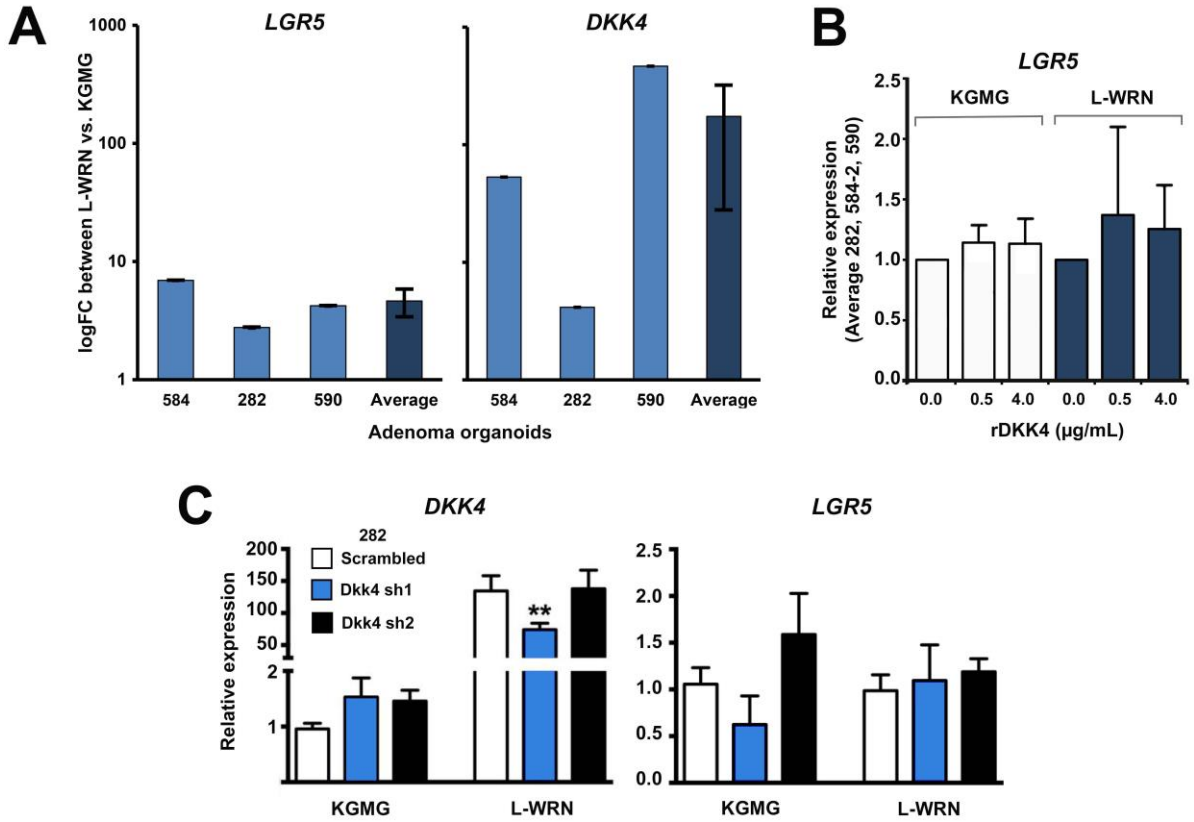

Figure 7. DKK4 (dickkopf WNT signaling pathway inhibitor-4) comparisons to LGR5 expression. **(A)** Relative *LGR5* and *DKK4* mRNA expression in L-WRN vs KGMG cultures. Individual specimen standard error as technical replicates, n=6; with average and SE values of the three biological replicates. **(B)** *LGR5* mRNA expression levels in adenoma organoids after treatment for 72 hrs with recombinant DKK4 in KGMG and L-WRN. **(C)** *DKK4* and *LGR5* expression levels in stable adenoma organoids with two *DKK4* knockdowns (Dkk4 sh1, Dkk4 sh2) and scramble small hairpin RNA (scramble).

bioRxiv preprint doi: https://doi.org/10.1101/118034; this version posted March 18, 2017. The copyright holder for this preprint (which was not certified by peer review) is the author/funder, who has granted bioRxiv a license to display the preprint in perpetuity. It is made available under aCC-BY 4.0 International license.

Identification and Isolation of Normal Colon LGR5(+) Cells

Due to the enrichment of LGR5(+) cells grown in media promoting high-WNT signaling levels, we also wanted to isolate LGR5(+) cells directly from normal colon tissue to demonstrate robustness of the isolation and purification methods. Using the same dissociation methods as were employed for the adenoma organoid cultures, dissociated single cells from 3 independent normal cadaveric colon specimens were sorted for EpCAM positivity and LGR5 expression. LGR5(+) cells comprised 2.35%, 0.63%, and 0.76% of the EpCAM(+) cells in independent experiments. A representative distribution of LGR5(+) staining from a normal colon, demonstrates that fluorescent intensity for LGR5(+) events were 2-3 orders of magnitude above baseline (Figure 8A). LGR5(+) cells were collected and subsequently analyzed by qPCR for *LGR5* and the intestinal stem cell marker *OLFM4*, which was recently shown to be expressed in normal human colon, and in adenoma (Jang et al. 2016). We identified an average of 7.5-fold increase in *LGR5* expression and 2.3-fold increase in *OLFM4* mRNA expression in the sorted LGR5(+) normal colon cells relative to the LGR5(-) cells (Figure 8B). Further, protein expression of OLFM4 was confirmed by IF, which showed staining at the bottom 1/3rd of the normal colon crypts (Figure 8C).

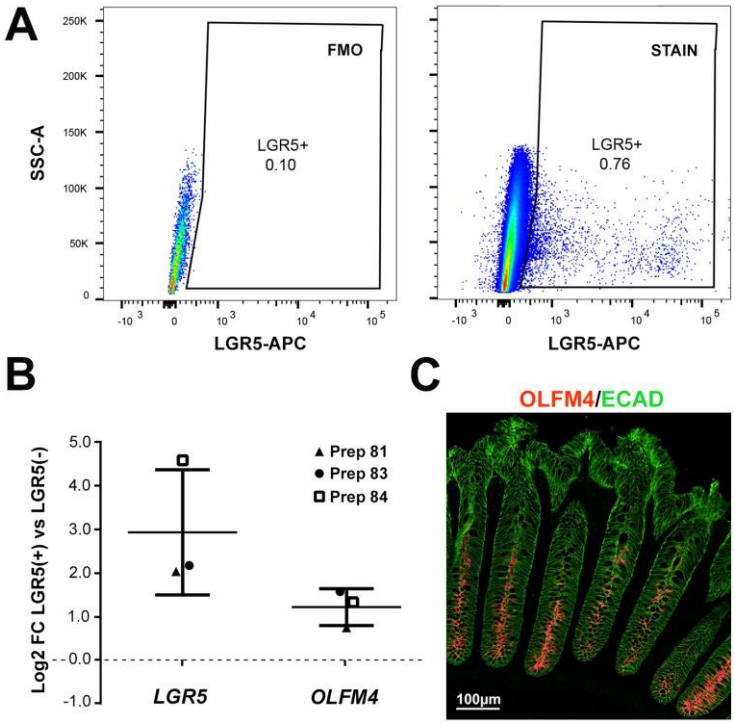

Figure 8. Identification, isolation and culture of patient-derived normal colon LGR5(+) cells. (A) Flow cytometry gating strategy for LGR5(+) cells isolated directly from warm autopsy normal colon tissue (representative scatter plots of 3 specimens; specimen 84). Includes EpCAM(+) inclusion criteria, using a phycoerythrin (PE)-conjugated antibody (not shown). To set the LGR5-APC(+) gating, either magnet flow-through (specimen 81 & 83), as done with organoid sorts, or rigorous so-called fluorescence-minus-one controls [FMO; DAPI(-), EpCAM(+);specimen 84] were used. **(B)** mRNA expression by qPCR of *LGR5* and *OLFM4* across all 3 patient samples. **(C)** OLFM4 immunofluorescent staining of normal colon crypts.

bioRxiv preprint doi: https://doi.org/10.1101/118034; this version posted March 18, 2017. The copyright holder for this preprint (which was not certified by peer review) is the author/funder, who has granted bioRxiv a license to display the preprint in perpetuity. It is made available under aCC-BY 4.0 International license.

DISCUSSION

LGR5 has been identified as one of the few cell surface markers available for the identification and isolation of cycling stem cells in the colonic crypt, although efforts to generate effective antibodies to isolate these cells have largely been unsuccessful.(Barker 2014). Recently antibody drug conjugates (ADCs) have been developed to target cells expressing LGR5, demonstrating therapeutic potential (Gong et al. 2016, Junttila et al. 2015), but as part of these applications primary human cell isolation and characterization was limited (Hirsch and Ried 2016). Thus, the role of LGR5(+) stem cells in human intestinal development, homeostasis, and carcinogenesis remains poorly understood. The identification and isolation of human LGR5(+) adenoma cells, as well as the establishment of methods for the long term culture and propagation of organoids enriched for these rare cells, as described in this study, provides some of the first insight into the characteristics of these cells in humans. Further, we confirm that our methods are robust for the identification and isolation of LGR5(+) cells from normal human colon tissues. Ideally, methods and data sets presented in this work will be widely utilized to overcome a major hurdle in the field of colorectal cancer stem cell biology.

Human primary intestinal organoid culture systems represent an unparalleled tool to study colorectal cancer biology (Matano et al. 2015) and to develop precision medicine platforms for targeted therapeutics (van de Wetering et al. 2015). Here, we report a living biobank of human normal colon, adenoma, and adenocarcinoma tissues. We used this biobank to study and isolate LGR5(+) cells from four genetically diverse adenoma-derived organoids. We found that LGR5 is expressed at higher levels in organoids in response to Wnt3a, Rspondin-3, and Noggin, and that this is associated with a cystic phenotype, consistent with other reports (Sato, van Es, et al. 2011, Farin, Van Es, and Clevers 2012, Matano et al. 2015, Drost et al. 2015, Onuma et al. 2013). While this report was in preparation, a study eloquently demonstrated that Mex3a marks a subset of Lgr5(+) slow cycling intestinal cells (Barriga et al. 2017). Indeed, we show that *MEX3A* is among the upregulated genes in isolated human colon LGR5(+) cells. Interestingly, while gene expression associated with LGR5 expression in human adenoma significantly overlapped with *Lgr5*^{HI} stem cells in the mouse (Munoz et al. 2012), there were several interesting examples where human expression patterns were

bioRxiv preprint doi: https://doi.org/10.1101/118034; this version posted March 18, 2017. The copyright holder for this preprint (which was not certified by peer review) is the author/funder, who has granted bioRxiv a license to display the preprint in perpetuity. It is made available under aCC-BY 4.0 International license.

opposite to that of the mouse. For example, *SEMA3B* and *PLCE1* are enriched in mouse *Lgr5*^{HI} cells, but were downregulated (FDR=0.04 and 0.002 respectively) in human LGR5(+) adenoma cells. Determining whether differential expression of these genes reflects differences in human compared to mouse biology or adenoma compared to normal human colon biology represents an important future direction for this research.

Histological approaches that compared LGR5(+) cells from adenoma and adenocarcinoma samples with normal colon revealed a number of unexpected biological findings. For example, we identified the presence of stromal LGR5 staining, and confirmed the specificity of this signal with *LGR5* mRNA ISH. We did not however identify obvious stromal staining in normal tissue. We identified that stromal staining of LGR5 was associated with cancer stage based on a cohort of independent samples on a tissue microarray. Others have identified the presence of multipotent Lgr5(+) stromal cells in the oral mucosa and tongue of adult mice expressing the Lgr5-EGFP reporter with a phenotype resembling neural crest cells (Boddupally et al. 2016). Our finding is likely of high relevance in light of the identification of stromal gene expression having a strong correlation with colorectal cancer subtypes (Calon et al. 2015). Future work should focus on understanding the role of these putative LGR5 expressing stromal cells in colorectal carcinogenesis.

Transcriptional comparisons of LGR5(+) adenoma stem cells with published normal colonic RNA-seq data (Uhlen et al. 2015), identified genes strongly upregulated in LGR5(+) adenoma cells that were virtually unexpressed in the normal human colon: *DKK4* and *FGF20*. *DKK4* is a negative regulator of Wnt signaling that has been reported as both upregulated (Matsui et al. 2009, Pendas-Franco et al. 2008) and downregulated in CRC (Baehs et al. 2009). A recent study showed that DKK4 acts selectively to inhibit a subset of WNT ligands, but is proteolytically inactivated (Sima et al. 2016). Elevated *DKK4* expression is linked with CRC chemoresistance (Ebert et al. 2012) and metastasis (Chen et al. 2015), both processes associated with cancer stem cells. *DKK4* expression has also been correlated with *FGF20* expression (Matsui et al. 2009), and *FGF20* is a known Wnt target gene (Katoh and Katoh 2007), although the role that FGF20 plays in colorectal carcinogenesis is not well defined. We identified that *DKK4* and *FGF20* are significantly upregulated in colorectal cancers, compared to normal colon, in data from TCGA. The knockdown of *DKK4*, or treatment of organoids with recombinant DKK4, did not modulate *LGR5* expression, calling into question

bioRxiv preprint doi: https://doi.org/10.1101/118034; this version posted March 18, 2017. The copyright holder for this preprint (which was not certified by peer review) is the author/funder, who has granted bioRxiv a license to display the preprint in perpetuity. It is made available under aCC-BY 4.0 International license.

whether there is a functional role for DKK4 in LGR5(+) cells. However, the association with *LGR5* expression suggests that DKK4 could be a novel biomarker of colon adenoma stem cells or cells with high Wnt activity, and may prove useful for colon cancer prevention or treatment efforts.

Notably, our experiments used a two-step enrichment methodology to obtain purified cells (magnet followed by FACS), yet we still encountered a relatively small population of LGR5(+) cells. This could be explained, in part, by work showing rapid internalization of LGR5 from the plasma membrane to the trans-golgi network (Snyder et al. 2017). Thus, it is possible that our antibody-based methods will only recognize rare cells expressing the highest levels of LGR5 protein on the cell surface. On one hand, this may preclude us from isolating cells that express *LGR5* mRNA but that do not have abundant protein localized to the cell surface. On the other hand, this same caveat would enhance specificity for the sorted population of cells, as supported by our gene expression profiling.

Our study presents a blueprint for the identification, *in vitro* culture, isolation, and experimental characterization of human LGR5(+) cells. We anticipate our methods can be readily adapted for the isolation and characterization of the LGR5(+) cell populations in other human tissues including stomach (Barker et al. 2010, Simon et al. 2012), hair (Jaks et al. 2008), mammary gland (de Visser et al. 2012), prostate (Wang, Wang, et al. 2015), and kidney (Barker et al. 2012). Additionally, we expect that the organoid culture methods described here will provide an experimental platform for the development of novel chemopreventive and chemotherapeutic agents that target LGR5(+) stem cells.

bioRxiv preprint doi: https://doi.org/10.1101/118034; this version posted March 18, 2017. The copyright holder for this preprint (which was not certified by peer review) is the author/funder, who has granted bioRxiv a license to display the preprint in perpetuity. It is made available under aCC-BY 4.0 International license.

REFERENCES

Agorku, David, Greg Parker, Nadine Chelius, Andreas Bosio, and Olaf Hardt. *Novel monoclonal antibodies for the analysis and isolation of Lgr5-positive cells* 2013 [cited 13 March 2017. Available from https://www.miltenyibiotec.com/~/media/Images/Products/Import/0009400/IM0009476.ashx.

Agorku, David, Greg Parker, Nadine Chelius, Andreas Bosio, and Olaf Hardt. 2014. "Abstract 3757: Novel monoclonal antibodies for the analysis and isolation of Lgr5 positive cells." *Cancer Research* no. 73 (8 Supplement):3757. doi: 10.1158/1538-7445.AM2013-3757.

Baehs, S., A. Herbst, S. E. Thieme, C. Perschl, A. Behrens, S. Scheel, A. Jung, T. Brabletz, B. Goke, H. Blum, and F. T. Kolligs. 2009. "Dickkopf-4 is frequently down-regulated and inhibits growth of colorectal cancer cells." *Cancer Lett* no. 276 (2):152-9. doi: 10.1016/j.canlet.2008.11.003.

Baker, A. M., T. A. Graham, G. Elia, N. A. Wright, and M. Rodriguez-Justo. 2015. "Characterization of LGR5 stem cells in colorectal adenomas and carcinomas." *Sci Rep* no. 5:8654. doi: 10.1038/srep08654.

Barker, N. 2014. "Adult intestinal stem cells: critical drivers of epithelial homeostasis and regeneration." *Nat Rev Mol Cell Biol* no. 15 (1):19-33. doi: 10.1038/nrm3721.

Barker, N., M. Huch, P. Kujala, M. van de Wetering, H. J. Snippert, J. H. van Es, T. Sato, D. E. Stange, H. Begthel, M. van den Born, E. Danenberg, S. van den Brink, J. Korving, A. Abo, P. J. Peters, N. Wright, R. Poulsom, and H. Clevers. 2010. "Lgr5(+ve) stem cells drive self-renewal in the stomach and build long-lived gastric units in vitro." *Cell Stem Cell* no. 6 (1):25-36. doi: 10.1016/j.stem.2009.11.013.

Barker, N., M. B. Rookmaaker, P. Kujala, A. Ng, M. Leushacke, H. Snippert, M. van de Wetering, S. Tan, J. H. Van Es, M. Huch, R. Poulsom, M. C. Verhaar, P. J. Peters, and H. Clevers. 2012. "Lgr5(+ve) stem/progenitor cells contribute to nephron formation during kidney development." *Cell Rep* no. 2 (3):540-52. doi: 10.1016/j.celrep.2012.08.018.

Barker, N., M. van de Wetering, and H. Clevers. 2008. "The intestinal stem cell." *Genes Dev* no. 22 (14):1856-64. doi: 10.1101/gad.1674008.

Barker, N., J. H. van Es, J. Kuipers, P. Kujala, M. van den Born, M. Cozijnsen, A. Haegebarth, J. Korving, H. Begthel, P. J. Peters, and H. Clevers. 2007. "Identification of stem cells in small intestine and colon by marker gene Lgr5." *Nature* no. 449 (7165):1003-7. doi: nature06196 [pii]10.1038/nature06196.

Barriga, F. M., E. Montagni, M. Mana, M. Mendez-Lago, X. Hernando-Momblona, M. Sevillano, A. Guillaumet-Adkins, G. Rodriguez-Esteban, S. J. Buczacki, M. Gut, H. Heyn, D. J. Winton, O. H. Yilmaz, C. S. Attolini, I. Gut, and E. Batlle. 2017. "Mex3a Marks a Slowly Dividing Subpopulation of Lgr5+ Intestinal Stem Cells." *Cell Stem Cell*. doi: 10.1016/j.stem.2017.02.007.

Becker, L., Q. Huang, and H. Mashimo. 2008. "Immunostaining of Lgr5, an intestinal stem cell marker, in normal and premalignant human gastrointestinal tissue." *ScientificWorldJournal* no. 8:1168-76. doi: 10.1100/tsw.2008.148.

Boddupally, K., G. Wang, Y. Chen, and A. Kobielak. 2016. "Lgr5 Marks Neural Crest Derived Multipotent Oral Stromal Stem Cells." *Stem Cells* no. 34 (3):720-31. doi: 10.1002/stem.2314.

Calon, A., E. Lonardo, A. Berenguer-Llergo, E. Espinet, X. Hernando-Momblona, M. Iglesias, M. Sevillano, S. Palomo-Ponce, D. V. Tauriello, D. Byrom, C. Cortina, C. Morral, C. Barcelo, S. Tosi, A. Riera, C. S. Attolini, D. Rossell, E. Sancho, and E. Batlle. 2015. "Stromal gene expression defines poor-prognosis subtypes in colorectal cancer." *Nat Genet* no. 47 (4):320-9. doi: 10.1038/ng.3225.

bioRxiv preprint doi: https://doi.org/10.1101/118034; this version posted March 18, 2017. The copyright holder for this preprint (which was not certified by peer review) is the author/funder, who has granted bioRxiv a license to display the preprint in perpetuity. It is made available under aCC-BY 4.0 International license.

Carmon, K. S., Q. Lin, X. Gong, A. Thomas, and Q. Liu. 2012. "LGR5 interacts and cointernalizes with Wnt receptors to modulate Wnt/beta-catenin signaling." *Mol Cell Biol* no. 32 (11):2054-64. doi: 10.1128/mcb.00272-12.

Chen, H. J., J. Sun, Z. Huang, H. Hou, Jr., M. Arcilla, N. Rakhilin, D. J. Joe, J. Choi, P. Gadamsetty, J. Milsom, G. Nandakumar, R. Longman, X. K. Zhou, R. Edwards, J. Chen, K. Y. Chen, P. Bu, L. Wang, Y. Xu, R. Munroe, C. Abratte, A. D. Miller, Z. H. Gumus, M. Shuler, N. Nishimura, W. Edelmann, X. Shen, and S. M. Lipkin. 2015. "Comprehensive models of human primary and metastatic colorectal tumors in immunodeficient and immunocompetent mice by chemokine targeting." *Nat Biotechnol* no. 33 (6):656-60. doi: 10.1038/nbt.3239.

Dame, M. K., Y. Jiang, H. D. Appelman, K. D. Copley, S. D. McClintock, M. N. Aslam, D. Attili, B. J. Elmunzer, D. E. Brenner, J. Varani, and D. K. Turgeon. 2014. "Human colonic crypts in culture: segregation of immunochemical markers in normal versus adenoma-derived." *Lab Invest* no. 94 (2):222-34. doi: 10.1038/labinvest.2013.145.

de Lau, W., N. Barker, T. Y. Low, B. K. Koo, V. S. Li, H. Teunissen, P. Kujala, A. Haegebarth, P. J. Peters, M. van de Wetering, D. E. Stange, J. E. van Es, D. Guardavaccaro, R. B. Schasfoort, Y. Mohri, K. Nishimori, S. Mohammed, A. J. Heck, and H. Clevers. 2011. "Lgr5 homologues associate with Wnt receptors and mediate R-spondin signalling." *Nature* no. 476 (7360):293-7. doi: 10.1038/nature10337.

de Visser, K. E., M. Ciampricotti, E. M. Michalak, D. W. Tan, E. N. Speksnijder, C. S. Hau, H. Clevers, N. Barker, and J. Jonkers. 2012. "Developmental stage-specific contribution of LGR5(+) cells to basal and luminal epithelial lineages in the postnatal mammary gland." *J Pathol* no. 228 (3):300-9. doi: 10.1002/path.4096.

Dedhia, P. H., N. Bertaux-Skeirik, Y. Zavros, and J. R. Spence. 2016. "Organoid Models of Human Gastrointestinal Development and Disease." *Gastroenterology* no. 150 (5):1098-112. doi: 10.1053/j.gastro.2015.12.042.

Drost, J., R. H. van Jaarsveld, B. Ponsioen, C. Zimberlin, R. van Boxtel, A. Buijs, N. Sachs, R. M. Overmeer, G. J. Offerhaus, H. Begthel, J. Korving, M. van de Wetering, G. Schwank, M. Logtenberg, E. Cuppen, H. J. Snippert, J. P. Medema, G. J. Kops, and H. Clevers. 2015. "Sequential cancer mutations in cultured human intestinal stem cells." *Nature* no. 521 (7550):43-7. doi: 10.1038/nature14415.

Ebert, M. P., M. Tanzer, B. Balluff, E. Burgermeister, A. K. Kretzschmar, D. J. Hughes, R. Tetzner, C. Lofton-Day, R. Rosenberg, A. C. Reinacher-Schick, K. Schulmann, A. Tannapfel, R. Hofheinz, C. Rocken, G. Keller, R. Langer, K. Specht, R. Porschen, J. Stohlmacher-Williams, T. Schuster, P. Strobel, and R. M. Schmid. 2012. "TFAP2E-DKK4 and chemoresistance in colorectal cancer." *N Engl J Med* no. 366 (1):44-53. doi: 10.1056/NEJMoa1009473.

Fan, X. S., H. Y. Wu, H. P. Yu, Q. Zhou, Y. F. Zhang, and Q. Huang. 2010. "Expression of Lgr5 in human colorectal carcinogenesis and its potential correlation with beta-catenin." *Int J Colorectal Dis* no. 25 (5):583-90. doi: 10.1007/s00384-010-0903-z.

Farin, H. F., J. H. Van Es, and H. Clevers. 2012. "Redundant sources of Wnt regulate intestinal stem cells and promote formation of Paneth cells." *Gastroenterology* no. 143 (6):1518-1529 e7. doi: 10.1053/j.gastro.2012.08.031.

Finkbeiner, S. R., D. R. Hill, C. H. Altheim, P. H. Dedhia, M. J. Taylor, Y. H. Tsai, A. M. Chin, M. M. Mahe, C. L. Watson, J. J. Freeman, R. Nattiv, M. Thomson, O. D. Klein, N. F. Shroyer, M. A. Helmrath, D. H. Teitelbaum, P. J. Dempsey, and J. R. Spence. 2015. "Transcriptome-wide Analysis Reveals Hallmarks of Human Intestine Development and Maturation In Vitro and In Vivo." *Stem Cell Reports*. doi: 10.1016/j.stemcr.2015.04.010.

bioRxiv preprint doi: https://doi.org/10.1101/118034; this version posted March 18, 2017. The copyright holder for this preprint (which was not certified by peer review) is the author/funder, who has granted bioRxiv a license to display the preprint in perpetuity. It is made available under aCC-BY 4.0 International license.

Gong, X., A. Azhdarinia, S. C. Ghosh, W. Xiong, Z. An, Q. Liu, and K. S. Carmon. 2016. "LGR5-Targeted Antibody-Drug Conjugate Eradicates Gastrointestinal Tumors and Prevents Recurrence." *Mol Cancer Ther* no. 15 (7):1580-90. doi: 10.1158/1535-7163.mct-16-0114.

Hirsch, Daniela, and Thomas Ried. 2016. "Targeting colorectal cancer (stem-like) cells using LGR5 directed antibody drug conjugates." *Annals of Translational Medicine* no. 4 (24):508. doi: 10.21037/atm.2016.11.78.

Jaks, V., N. Barker, M. Kasper, J. H. van Es, H. J. Snippert, H. Clevers, and R. Toftgard. 2008. "Lgr5 marks cycling, yet long-lived, hair follicle stem cells." *Nat Genet* no. 40 (11):1291-9. doi: 10.1038/ng.239.

Jang, B. G., H. S. Kim, K. J. Kim, Y. Y. Rhee, W. H. Kim, and G. H. Kang. 2016. "Distribution of intestinal stem cell markers in colorectal precancerous lesions." *Histopathology* no. 68 (4):567-77. doi: 10.1111/his.12787.

Jang, B. G., B. L. Lee, and W. H. Kim. 2013. "Distribution of LGR5+ cells and associated implications during the early stage of gastric tumorigenesis." *PLoS One* no. 8 (12):e82390. doi: 10.1371/journal.pone.0082390.

Junttila, M. R., W. Mao, X. Wang, B. E. Wang, T. Pham, J. Flygare, S. F. Yu, S. Yee, D. Goldenberg, C. Fields, J. Eastham-Anderson, M. Singh, R. Vij, J. A. Hongo, R. Firestein, M. Schutten, K. Flagella, P. Polakis, and A. G. Polson. 2015. "Targeting LGR5+ cells with an antibody-drug conjugate for the treatment of colon cancer." *Sci Transl Med* no. 7 (314):314ra186. doi: 10.1126/scitranslmed.aac7433.

Katoh, Y., and M. Katoh. 2007. "Conserved POU-binding site linked to SP1-binding site within FZD5 promoter: Transcriptional mechanisms of FZD5 in undifferentiated human ES cells, fetal liver/spleen, adult colon, pancreatic islet, and diffuse-type gastric cancer." *Int J Oncol* no. 30 (3):751-5.

Kemper, K., P. R. Prasetyanti, W. De Lau, H. Rodermond, H. Clevers, and J. P. Medema. 2012. "Monoclonal antibodies against Lgr5 identify human colorectal cancer stem cells." *Stem Cells* no. 30 (11):2378-86. doi: 10.1002/stem.1233.

Kleist, B., L. Xu, G. Li, and C. Kersten. 2011. "Expression of the adult intestinal stem cell marker Lgr5 in the metastatic cascade of colorectal cancer." *Int J Clin Exp Pathol* no. 4 (4):327-35.

Kobayashi, S., H. Yamada-Okabe, M. Suzuki, O. Natori, A. Kato, K. Matsubara, Y. Jau Chen, M. Yamazaki, S. Funahashi, K. Yoshida, E. Hashimoto, Y. Watanabe, H. Mutoh, M. Ashihara, C. Kato, T. Watanabe, T. Yoshikubo, N. Tamaoki, T. Ochiya, M. Kuroda, A. J. Levine, and T. Yamazaki. 2012. "LGR5-positive colon cancer stem cells interconvert with drug-resistant LGR5-negative cells and are capable of tumor reconstitution." *Stem Cells* no. 30 (12):2631-44. doi: 10.1002/stem.1257.

Matano, M., S. Date, M. Shimokawa, A. Takano, M. Fujii, Y. Ohta, T. Watanabe, T. Kanai, and T. Sato. 2015. "Modeling colorectal cancer using CRISPR-Cas9-mediated engineering of human intestinal organoids." *Nat Med* no. 21 (3):256-62. doi: 10.1038/nm.3802.

Matsui, A., T. Yamaguchi, S. Maekawa, C. Miyazaki, S. Takano, T. Uetake, T. Inoue, M. Otaka, H. Otsuka, T. Sato, A. Yamashita, Y. Takahashi, and N. Enomoto. 2009. "DICKKOPF-4 and -2 genes are upregulated in human colorectal cancer." *Cancer Sci* no. 100 (10):1923-30. doi: 10.1111/j.1349-7006.2009.01272.x.

bioRxiv preprint doi: https://doi.org/10.1101/118034; this version posted March 18, 2017. The copyright holder for this preprint (which was not certified by peer review) is the author/funder, who has granted bioRxiv a license to display the preprint in perpetuity. It is made available under aCC-BY 4.0 International license.

Miyoshi, Hiroyuki, and Thaddeus S. Stappenbeck. 2013. "In vitro expansion and genetic modification of gastrointestinal stem cells in spheroid culture." *Nat. Protocols* no. 8 (12):2471-2482. doi: 10.1038/nprot.2013.153 http://www.nature.com/nprot/journal/v8/n12/abs/nprot.2013.153.html#supplementary-information.

Montgomery, R. K., D. L. Carlone, C. A. Richmond, L. Farilla, M. E. Kranendonk, D. E. Henderson, N. Y. Baffour-Awuah, D. M. Ambruzs, L. K. Fogli, S. Algra, and D. T. Breault. 2011. "Mouse telomerase reverse transcriptase (mTert) expression marks slowly cycling intestinal stem cells." *Proc Natl Acad Sci U S A* no. 108 (1):179-84. doi: 1013004108 [pii] 10.1073/pnas.1013004108.

Munoz, J., D. E. Stange, A. G. Schepers, M. van de Wetering, B. K. Koo, S. Itzkovitz, R. Volckmann, K. S. Kung, J. Koster, S. Radulescu, K. Myant, R. Versteeg, O. J. Sansom, J. H. van Es, N. Barker, A. van Oudenaarden, S. Mohammed, A. J. Heck, and H. Clevers. 2012. "The Lgr5 intestinal stem cell signature: robust expression of proposed quiescent '+4' cell markers." *EMBO J* no. 31 (14):3079-91. doi: 10.1038/emboj.2012.166 emboj2012166 [pii].

Onuma, K., M. Ochiai, K. Orihashi, M. Takahashi, T. Imai, H. Nakagama, and Y. Hippo. 2013. "Genetic reconstitution of tumorigenesis in primary intestinal cells." *Proc Natl Acad Sci U S A* no. 110 (27):11127-32. doi: 10.1073/pnas.1221926110.

Pendas-Franco, N., J. M. Garcia, C. Pena, N. Valle, H. G. Palmer, M. Heinaniemi, C. Carlberg, B. Jimenez, F. Bonilla, A. Munoz, and J. M. Gonzalez-Sancho. 2008. "DICKKOPF-4 is induced by TCF/beta-catenin and upregulated in human colon cancer, promotes tumour cell invasion and angiogenesis and is repressed by 1alpha,25-dihydroxyvitamin D3." *Oncogene* no. 27 (32):4467-77. doi: 10.1038/onc.2008.88.

Powell, A. E., Y. Wang, Y. Li, E. J. Poulin, A. L. Means, M. K. Washington, J. N. Higginbotham, A. Juchheim, N. Prasad, S. E. Levy, Y. Guo, Y. Shyr, B. J. Aronow, K. M. Haigis, J. L. Franklin, and R. J. Coffey. 2012. "The pan-ErbB negative regulator Lrig1 is an intestinal stem cell marker that functions as a tumor suppressor." *Cell* no. 149 (1):146-58. doi: S0092-8674(12)00280-2 [pii] 10.1016/j.cell.2012.02.042.

Sato, T., D. E. Stange, M. Ferrante, R. G. Vries, J. H. Van Es, S. Van den Brink, W. J. Van Houdt, A. Pronk, J. Van Gorp, P. D. Siersema, and H. Clevers. 2011. "Long-term expansion of epithelial organoids from human colon, adenoma, adenocarcinoma, and Barrett's epithelium." *Gastroenterology* no. 141 (5):1762-72. doi: S0016-5085(11)01108-5 [pii] 10.1053/j.gastro.2011.07.050.

Sato, T., J. H. van Es, H. J. Snippert, D. E. Stange, R. G. Vries, M. van den Born, N. Barker, N. F. Shroyer, M. van de Wetering, and H. Clevers. 2011. "Paneth cells constitute the niche for Lgr5 stem cells in intestinal crypts." *Nature* no. 469 (7330):415-8. doi: 10.1038/nature09637 nature09637 [pii].

Sato, T., R. G. Vries, H. J. Snippert, M. van de Wetering, N. Barker, D. E. Stange, J. H. van Es, A. Abo, P. Kujala, P. J. Peters, and H. Clevers. 2009. "Single Lgr5 stem cells build crypt-villus structures in vitro without a mesenchymal niche." *Nature* no. 459 (7244):262-5. doi: 10.1038/nature07935 nature07935 [pii].

Schepers, Arnout G., Hugo J. Snippert, Daniel E. Stange, Maaike van den Born, Johan H. van Es, Marc van de Wetering, and Hans Clevers. 2012. "Lineage Tracing Reveals Lgr5+ Stem Cell Activity in Mouse Intestinal Adenomas." *Science* no. 337 (6095):730-735. doi: 10.1126/science.1224676.

Sima, J., Y. Piao, Y. Chen, and D. Schlessinger. 2016. "Molecular dynamics of Dkk4 modulates Wnt action and regulates Meibomian gland development." *Development*. doi: 10.1242/dev.143909.

Simon, E., D. Petke, C. Boger, H. M. Behrens, V. Warneke, M. Ebert, and C. Rocken. 2012. "The spatial distribution of LGR5+ cells correlates with gastric cancer progression." *PLoS One* no. 7 (4):e35486. doi: 10.1371/journal.pone.0035486.

bioRxiv preprint doi: https://doi.org/10.1101/118034; this version posted March 18, 2017. The copyright holder for this preprint (which was not certified by peer review) is the author/funder, who has granted bioRxiv a license to display the preprint in perpetuity. It is made available under aCC-BY 4.0 International license.

Snippert, H. J., L. G. van der Flier, T. Sato, J. H. van Es, M. van den Born, C. Kroon-Veenboer, N. Barker, A. M. Klein, J. van Rheenen, B. D. Simons, and H. Clevers. 2010. "Intestinal crypt homeostasis results from neutral competition between symmetrically dividing Lgr5 stem cells." *Cell* no. 143 (1):134-44. doi: 10.1016/j.cell.2010.09.016.

Snyder, J. C., L. K. Rochelle, C. Ray, T. F. Pack, C. B. Bock, V. Lubkov, H. K. Lyerly, A. S. Waggoner, L. S. Barak, and M. G. Caron. 2017. "Inhibiting clathrin-mediated endocytosis of the leucine-rich G protein-coupled Receptor-5 diminishes cell fitness." *J Biol Chem*. doi: 10.1074/jbc.M116.756635.

Takahashi, H., H. Ishii, N. Nishida, I. Takemasa, T. Mizushima, M. Ikeda, T. Yokobori, K. Mimori, H. Yamamoto, M. Sekimoto, Y. Doki, and M. Mori. 2011. "Significance of Lgr5(+ve) cancer stem cells in the colon and rectum." *Ann Surg Oncol* no. 18 (4):1166-74. doi: 10.1245/s10434-010-1373-9.

The Cancer Genome Atlas, Network. 2012. "Comprehensive Molecular Characterization of Human Colon and Rectal Cancer." *Nature* no. 487 (7407):330-337. doi: 10.1038/nature11252.

Uhlen, M., L. Fagerberg, B. M. Hallstrom, C. Lindskog, P. Oksvold, A. Mardinoglu, A. Sivertsson, C. Kampf, E. Sjostedt, A. Asplund, I. Olsson, K. Edlund, E. Lundberg, S. Navani, C. A. Szigyarto, J. Odeberg, D. Djureinovic, J. O. Takanen, S. Hober, T. Alm, P. H. Edqvist, H. Berling, H. Tegel, J. Mulder, J. Rockberg, P. Nilsson, J. M. Schwenk, M. Hamsten, K. von Feilitzen, M. Forsberg, L. Persson, F. Johansson, M. Zwahlen, G. von Heijne, J. Nielsen, and F. Ponten. 2015. "Proteomics. Tissue-based map of the human proteome." *Science* no. 347 (6220):1260419. doi: 10.1126/science.1260419.

van de Wetering, M., H. E. Francies, J. M. Francis, G. Bounova, F. Iorio, A. Pronk, W. van Houdt, J. van Gorp, A. Taylor-Weiner, L. Kester, A. McLaren-Douglas, J. Blokker, S. Jaksani, S. Bartfeld, R. Volckman, P. van Sluis, V. S. Li, S. Seepo, C. Sekhar Pedamallu, K. Cibulskis, S. L. Carter, A. McKenna, M. S. Lawrence, L. Lichtenstein, C. Stewart, J. Koster, R. Versteeg, A. van Oudenaarden, J. Saez-Rodriguez, R. G. Vries, G. Getz, L. Wessels, M. R. Stratton, U. McDermott, M. Meyerson, M. J. Garnett, and H. Clevers. 2015. "Prospective derivation of a living organoid biobank of colorectal cancer patients." *Cell* no. 161 (4):933-45. doi: 10.1016/j.cell.2015.03.053.

van der Flier, L. G., A. Haegebarth, D. E. Stange, M. van de Wetering, and H. Clevers. 2009. "OLFM4 is a robust marker for stem cells in human intestine and marks a subset of colorectal cancer cells." *Gastroenterology* no. 137 (1):15-7. doi: 10.1053/j.gastro.2009.05.035.

Vermeulen, L., E. Melo F. De Sousa, M. van der Heijden, K. Cameron, J. H. de Jong, T. Borovski, J. B. Tuynman, M. Todaro, C. Merz, H. Rodermond, M. R. Sprick, K. Kemper, D. J. Richel, G. Stassi, and J. P. Medema. 2010. "Wnt activity defines colon cancer stem cells and is regulated by the microenvironment." *Nat Cell Biol* no. 12 (5):468-76. doi: 10.1038/ncb2048.

Wang, B. E., X. Wang, J. E. Long, J. Eastham-Anderson, R. Firestein, and M. R. Junttila. 2015. "Castration-resistant Lgr5(+) cells are long-lived stem cells required for prostatic regeneration." *Stem Cell Reports* no. 4 (5):768-79. doi: 10.1016/j.stemcr.2015.04.003.

Wang, X., Y. Yamamoto, L. H. Wilson, T. Zhang, B. E. Howitt, M. A. Farrow, F. Kern, G. Ning, Y. Hong, C. C. Khor, B. Chevalier, D. Bertrand, L. Wu, N. Nagarajan, F. A. Sylvester, J. S. Hyams, T. Devers, R. Bronson, D. B. Lacy, K. Y. Ho, C. P. Crum, F. McKeon, and W. Xian. 2015. "Cloning and variation of ground state intestinal stem cells." *Nature* no. 522 (7555):173-8. doi: 10.1038/nature14484.

Yan, K. S., L. A. Chia, X. Li, A. Ootani, J. Su, J. Y. Lee, N. Su, Y. Luo, S. C. Heilshorn, M. R. Amieva, E. Sangiorgi, M. R. Capecchi, and C. J. Kuo. 2012. "The intestinal stem cell markers Bmi1 and Lgr5 identify two functionally distinct populations." *Proc Natl Acad Sci U S A* no. 109 (2):466-71. doi: 10.1073/pnas.1118857109.

bioRxiv preprint doi: https://doi.org/10.1101/118034; this version posted March 18, 2017. The copyright holder for this preprint (which was not certified by peer review) is the author/funder, who has granted bioRxiv a license to display the preprint in perpetuity. It is made available under aCC-BY 4.0 International license.

Supplemental Experimental Procedures and Figures

Establishment of Organoid Cultures from Human Colonic Adenomas.

The isolation and culture procedure was based on recently described methodology for establishing and maintaining unlimited growth of human colonic adenoma tissue in organoid culture (Dame et al. 2014) founded in the original work of Sato *et al* (Sato, Stange, et al. 2011). Use of this procedure has generated a working cryorepository of adenoma organoids (Table S1). Tissue was collected from subjects recruited through the Molecular Pathology and Biosample Core (MPBC) as part of the GI SPORE at the University of Michigan. Colonic tissue was acquired by endoscopy (adenomas) or from colonic resections (adenocarcinomas) and according to protocols approved by the University of Michigan Institutional Review Board (IRB; HUM00064405/0038437/00030020). Adult small intestinal and colonic tissue was collected from deceased donors through the Gift of Life, Michigan (University of Michigan IRB HUM0010148810). Fetal small intestinal tissue was obtained from the University of Washington Laboratory of Developmental Biology and approved by University of Michigan under IRB approval (HUM00093465).

Two growth media were used. The patient-derived adenoma organoid specimens selected for this study were maintained in continuous culture in a reduced medium (KGM-Gold, 195769; Lonza, Walkersville, MD); a serum-free epithelial medium containing epidermal growth factor (EGF) and pituitary extract, with the antimicrobials 25µg/mL gentamicin (Gibco, #15750060; Grand Island, NY) and 50µg/mL Primocin (InvivoGen, #ant-pm-1; San Diego, CA) and made to 0.15mM calcium with $CaCl_2$ (PromoCell GmbH; # 34006; Heidelberg, Germany). The second medium (L-WRN medium) was employed to drive the budding organoids into a cystic morphology; high in Wnt3a, R-spondin-3 and Noggin, all provided by a conditioned medium from stably transfected support L-cells as described by Miyoshi (Miyoshi and Stappenbeck 2013). The complete L-WRN medium contained Advanced DMEM/F-12 (Gibco, 12634028), 2mM GlutaMax (Gibco, #35050-061), 10mM HEPES (Gibco, #15630080), N-2 media supplement (Gibco; #17502048), B-27 supplement minus vitamin A (Gibco; 12587010), 50 units/mL penicillin, 0.05 mg/mL streptomycin (Gibco, #15070063), 50µg/ml Primocin (InvivoGen; San Diego, CA), 1mM N-Acetyl-L-cysteine (Sigma-Aldrich, A9165; St. Louis, MO), and 100ng EGF/mL (R&D Systems, Inc., 236-EG;

bioRxiv preprint doi: https://doi.org/10.1101/118034; this version posted March 18, 2017. The copyright holder for this preprint (which was not certified by peer review) is the author/funder, who has granted bioRxiv a license to display the preprint in perpetuity. It is made available under aCC-BY 4.0 International license.

Minneapolis, MN), as well as the addition of 10mM Nicotinamide (Sigma-Aldrich, N0636). To drive the cultures to a cyst morphology, cultures were gradually switched from KGMG to L-WRN for three to four weeks (3 days KGMG post-passage, 5 days 50/50 L-WRN; 5 days 75/25; 100% L-WRN until predominately cystic). Consistent with previous reports, organoids formed cystic structures in the presence of Wnt ligand provided by L-WRN medium (Onuma et al. 2013, Drost et al. 2015, Sato, van Es, et al. 2011, Farin, Van Es, and Clevers 2012, Matano et al. 2015).

Growth of normal colon organoids and some adenoma specimens required the above L-WRN medium with additional growth factors: 10µM SB202190 (Sigma-Aldrich; S7067) and 500nM A83-01 (R&D Tocris, #2939) (Sato, Stange, et al. 2011). Further, a subset of these adenoma showed inhibition of growth with the p38 MAP kinase inhibitor, SB202190 (Sigma-Aldrich; #S7067), as described by Fujii et al (Fujii et al. 2016). 10mM Nicotinamide was used at the initial establishment of the specimens in organoid culture, and then removed for continued expansion.

Cultures were propagated in Matrigel (Corning, #354234; Bedford, MA) which was diluted to 8mg/mL in growth media on 6-well tissue culture plates (USA Scientific CytoOne, #CC7682-7506; Ocala, FL). All plasticware, excluding culture plates, were coated in 0.1% bovine serum albumen in DPBS (Sigma-Aldrich; #A8806) to prevent tissue/organoids/cells from adhering to surfaces. Cultures were passaged every 4-7 days by digesting Matrigel in cold 2mM EDTA in DPBS and plated the first day with the Rho-associated protein kinase (*ROCK*) inhibitor, 10µM Y27632 (Miltenyi Biotec GmbH, #130-104-169; Bergisch Gladbach, Germany). For normal colon and select adenoma grown in L-WRN, 2.5µM CHIR99021 (Miltenyi Biotec, #130-103-926) was also added at passaging.

Genomic Characterization of Organoid Cryorepository Specimens.

DNA was extracted from Allprotect Tissue Reagent (Qiagen, #76405; Germantown, MD) preserved samples or directly from fresh organoid preparations with the All prep DNA/RNA/protein mini kit (Qiagen, #80004). For specimens 574 and 584, DNA was isolated from FFPE source tumor with the QIAamp DNA FFPE Tissue Kit, (Qiagen, #56404).

bioRxiv preprint doi: https://doi.org/10.1101/118034; this version posted March 18, 2017. The copyright holder for this preprint (which was not certified by peer review) is the author/funder, who has granted bioRxiv a license to display the preprint in perpetuity. It is made available under aCC-BY 4.0 International license.

The QIAseq Targeted DNA colorectal cancer panel (Qiagen, #DHS-002Z) was used to determine the presence of somatic and germline variants (Figure 4B, Table 1). The panel is compatible with Illumina sequencing technology and covers 71 different oncogenes and tumor suppressor genes often mutated in colorectal cancers. The assay was performed using 80ng of purified gDNA following the vendor's manual. The libraries were sequenced on a HiSEQ 2500 using V2 chemistry (Illumina Inc; San Diego, CA). The sequencing data was demultiplexed and the Fastq files generated using Casava. The fastq files were imported into the QIAseq DNA enrichment portal for alignment and variant analysis. The targets were covered at an average read depth of 2000x with a coverage uniformity at 20% of the mean over 99%. Somatic variants were manually inspected in the integrative genomics viewer (IGV, Broad Institute). The variants of low quality or with an allele frequency below 5% were filtered out.

Whole exome sequencing was performed for specimens 590 and 14881. Briefly, DNA was fragmented to 250bp using standard Covaris sonication. Fragmented DNA was prepared as a standard Illumina gDNAlibrary using IntegenX reagents. Then the samples were PCR amplified, libraries were checked for quality and quantity. Samples then underwent exome capture (using the Roche Nimblegen SeqCap EZ v3.0 according to the manufacturer's protocols (Roche Nimblegen, Indianapolis, IN). The SeqCap EZ Human Exome Library v3.0 covers 64 Mb of coding exons and miRNAs. Captured libraries were sequenced on a HiSeq 2500 using 100 Cycle paired end reads. The exome sequencing data was analyzed by the variant calling pipeline developed by the University of Michigan Bioinformatics Core. For each of the samples, paired-end reads were aligned to the hg19 reference genome using BWA v0.7.8 (Li and Durbin 2009), followed by removal of sequence duplicates using PicardTools v1.79 (http://picard.sourceforge.net), local realignment around INDELs and base quality score recalibration using GATK v3.2-2 (DePristo et al. 2011). Read coverage on exome capture target regions was calculated using BEDTools v2.20.1 (Quinlan and Hall 2010). Normal-Tumor paired alignment files were submitted to MuTect v1.1.4 (Cibulskis et al. 2013), Strelka v1.0.14 (Saunders et al. 2012), and Varscan v2.3.7 (with its false-positive filter) (Koboldt et al. 2012) for the detection of somatic and germline SNPs and INDELs. Candidate variant calls across all samples and patients were merged using Jacquard (Gates et al. 2015) into a

bioRxiv preprint doi: https://doi.org/10.1101/118034; this version posted March 18, 2017. The copyright holder for this preprint (which was not certified by peer review) is the author/funder, who has granted bioRxiv a license to display the preprint in perpetuity. It is made available under aCC-BY 4.0 International license.

single VCF file that included all variant loci whose filter field passed in MuTect or Strelka or VarScan (VarScan calls were limited to somatic variants confirmed in false-positive filter). Variants were annotated using SnpEff v4.0/hg19 (Cingolani et al. 2012), dbNSFP v2.4 (Liu, Jian, and Boerwinkle 2011, 2013), dbSNP v138, and 1000 Genomes v3 (Abecasis et al. 2012). For variants associated with multiple effects or multiple transcripts, a single "top effect" annotation was nominated based on annotation confidence, predicted impact, gene region, and transcript length. Common variants (at or above 5% overall population allele frequency as reported by 1000 Genomes) were excluded. Subsequent variant calling was as follows: rejected Impact Ranks low & modifier and accepted high & moderate; rejected Population Category common; excluded dbNSFP when damaging was equal to zero for all nine data bases, and selected allelic frequency ≥ 0.15.

Further Specificity Studies of LGR5 Antibodies and Development of Procedures for Enrichment of LGR5(+) cells by Magnetic-activated Cell Sorting (MACS).

Mouse pre-B cell lymphoma 1881 cells transfected with his-tagged *LGR5* [1881(+)] or wild type [1881(-)] (provided by Miltenyi Biotec) were cultured in suspension in RPMI (Gibco, #21870-076) containing 20mM HEPES, 2mM L-glutamine, 10% FBS (Hyclone characterized, GE Healthcare Life Sciences , #SH30071.03; Marlborough, MA), 50 units/mL penicillin, 0.05 mg/mL streptomycin, 1mM sodium pyruvate (Gibco, #11360070), and 50µM β-mercaptoethanol (Gibco, #21985023). Transfected cells were selected using 15 µg/ml Blasticidin S (Gibco, #R210-01).

<u>*LGR5* quantitative real-time PCR of 1881 LGR5(+) and 1881 LGR5(-) cells</u>

To confirm transfection stability, the 1881 LGR5(+) and 1881 LGR5(-) cells were assayed for *LGR5*, and visualized with agarose gel analysis of qRT-PCR amplified products. mRNA expression of 1881 LGR5(+) and 1881 LGR5(-) cells was quantified by qRT-PCR (three biological replicates). Total RNA was extracted using TRIzol Reagent (Invitrogen, #15596-026; Carlsbad, CA) according to the manufacturer's recommendations. Complementary DNA was generated using TaqMan Reverse Transcription Reagents (Applied Biosystems, N808024; Carlsbad, CA). Quantitative real-time PCR was performed using Brilliant II

bioRxiv preprint doi: https://doi.org/10.1101/118034; this version posted March 18, 2017. The copyright holder for this preprint (which was not certified by peer review) is the author/funder, who has granted bioRxiv a license to display the preprint in perpetuity. It is made available under aCC-BY 4.0 International license.

SYBR Green Master Mix (Agilent technologies, #600828; Santa Clara, CA) on a StepOnePlus Real-Time PCR System (Applied Biosystems). All reactions were run with 40 cycles of 95°C for 10 minutes, 94°C for 30 seconds, 60°C for 30 seconds, and 72°C for 60 seconds, followed by a melt curve of 95°C for 10 seconds, 60°C for 1 minute and then increasing at 0.5 degree increments to 95°C. Gene expression analysis was normalized to the housekeeping gene *ACTB* and values were plotted as arbitrary units. The qRT-PCR amplified products (Figure 2B) were analyzed by running on a 1.5% Agarose gel (Bio-Rad Laboratories, #1620137; Hercules, California) to confirm the target amplicons size and to indicate that there were no non-specific amplification products. Primer sequences were as follows: *hLGR5* (Finkbeiner and Spence 2013): CAGCGTCTTCACCTCCTACC (Forward primer); TGGGAATGTATGTCAGAGCG (Reverse primer); 126 bp band size. *mACTB* (Riera et al. 2014): CTAAGGCCAACCGTGAAAAG (Forward primer); CCAGAGGCATACAGGGACA (Reverse primer); 104 bp band size.

Flow cytometry spike-in experiments

Cells were analyzed on a LSRII cytometer (BD Biosciences) to confirm LGR5 antibody specificity and validate the magnetic bead enrichment strategy (magnetic-activated cell sorting, MACS) (Figure S1B). 1881 LGR5(+) and wild type 1881 LGR5(-) cells were mixed at varying proportions and analyzed by flow cytometry before and after magnetic separation with rat monoclonal antibody anti-human LGR5 clone 22H2.8 conjugated to magnetic beads (Miltenyi Biotec, #130-104-072), with the allophycocyanin (APC) anti-bead check reagent conjugate to recognize the bound magnetic beads (Miltenyi Biotec, #130-098-892). Detailed flow cytometry/MACS methods are as described in the below methods section, “Single Cell Isolation and Magnetic separation for LGR5(+) and LGR5(-) cells”.

ImageStream Analysis

Cells were dissociated from adenoma organoid specimen 574 and stained with rat monoclonal antibody anti-human LGR5 clone 22H2.8 conjugated to phycoerythrin (PE) (2µg/mL; Miltenyi Biotec, #130-100-848). Dead cells were excluded using the Live/Dead Fixable Violet Dead Cell Stain Kit (405 nm excitation; Molecular Probes, #L34955; Eugene, Oregon). Gating strategy set the PE-positive cell population

bioRxiv preprint doi: https://doi.org/10.1101/118034; this version posted March 18, 2017. The copyright holder for this preprint (which was not certified by peer review) is the author/funder, who has granted bioRxiv a license to display the preprint in perpetuity. It is made available under aCC-BY 4.0 International license.

at 0.04% of the viable FMO-PE control with Rat IgG2b-PE (Thermo Fisher Scientific Ebioscience, #NC9634273; Waltham, MA). Cells were analyzed and imaged with the Amnis ImageStreamX Mark II (EMD Millipore; Kankakee, IL) for brightfield, SSC, and fluorescence. Analysis strategy follows: gradient RMS for focus, to intensity of MC 1 (Live-Dead) for viability, to intensity of MC 3 (PE) for rough positivity, to area channel 2 (fsc) vs. intensity channel 6 (ssc) for sizing to eliminate debris, to finally refined PE histogram. Samples were analyzed offline in the Amnis IDEAS software platform to generate images at 60x magnification (Figure 4E).

Western analysis

Whole-cell extracts were isolated, separated and transferred to nitrocellulose as previously described (Xue et al.). Cell lysates were prepared with the following: 150mM NaCl, 50mM Tris/ HCl pH8, 1% NP-40, 0.5% Triton-X 100, Protease inhibitor complete (Roche Life Science, # 04 693 116 001; Penzberg, Germany), fresh 2µg/mL aprotinin, fresh 10µg/mL leupeptin, fresh 100µg/mL PMSF, at 200µl buffer-mix per $1x10^7$ cells and incubated for 30 minutes on ice. Samples were centrifuged at 13,000xg for 15min at 4C and supernatant transferred to a fresh tube to determine the protein concentration (Bradford-assay). Before loading, samples were boiled for 5min at 95C. 15µg of sample protein was loaded to a Tris-Glycine 4-20% gradient gel (using Tris Glycine SDS running buffer). Protein was transferred to a nitrocellulose membrane and the membrane was blocked in TBS/Tween/milk powder (150mM NaCl; 50mM Tris pH 7,0; 0.1% Tween 20; 5% skim milk powder) for 1h at room temperature. The membrane was incubated with primary antibody 0.1µg/mL rabbit anti human LGR5 STE-1-89-11.5 (Miltenyi Biotec, #130-104-945) in 10mL TBS/Tween/milk powder overnight (shaking slightly) at 4°C, followed by 3X washes for 5min with TBS/Tween (150mM NaCl; 50mM Tris pH 7,0; 0.1% Tween 20) (shaking slightly). The membrane was incubated with secondary antibody (HRP goat anti rabbit IgG, 1:2000; Cell Signaling Technology; Boston, MA), diluted in 10mL TBS/Tween/milk powder for 1h at room temperature (shaking slightly), followed by 3X washes for 5min with TBS/Tween, 1X wash with deionized water for 5 minutes. The chemiluminescent signal was detected using Immobilon™ Western Kit (EMD Millipore) (Figure 2C).

bioRxiv preprint doi: https://doi.org/10.1101/118034; this version posted March 18, 2017. The copyright holder for this preprint (which was not certified by peer review) is the author/funder, who has granted bioRxiv a license to display the preprint in perpetuity. It is made available under aCC-BY 4.0 International license.

LGR5 Immunohistochemistry

Formalin fixed, paraffin sections were cut at 5-6 microns and rehydrated to water. Heat induced epitope retrieval was performed with FLEX TRS High pH Retrieval buffer (pH 9.01; Agilent Technologies, #K8004; Santa Clara, CA) for 20 minutes (Figure 1A, C and Figure 3A). After peroxidase blocking, the antibody LGR5 rabbit monoclonal clone STE-1-89-11.5 (Miltenyi Biotec, #130-104-945) was applied at a dilution of 1:50 (Figure 1A, C) or 1:100 (Figure 3A) at room temperature for 60 minutes. The FLEX HRP EnVision System (Agilent Technologies) was used for detection with a 10 minute DAB chromagen application. Slides were counterstained with Harris Hematoxylin for 5 seconds and then dehydrated and coverslipped (University of Michigan Comprehensive Cancer Center Tissue Core Research Histology and IHC Laboratory). Note, sections freshly cut were compared to those that were stored at room temperature for 4 weeks, and showed more robust LGR5 staining (data not shown). The colon cancer tissue microarray (TMA) (Figure 3A; 2 normal, 3 adenoma, 70 adenocarcinoma, 2 cores per specimen) was freshly cut and provided by BioChain Institute, Inc. (Newark, CA; Z7020032, lot B508131). Alternatively, retrieval was performed with R-Buffer B (pH 8.5; Electron Microscopy Sciences; Hatfield, PA) in a pressurized Retriever 2100 (Electron Microscopy Sciences) overnight (Figure 2A, Figure 4C). After peroxidase blocking, the antibody was applied at a dilution of 1:1000 at 4C overnight. ImmPACT DAB kit (Vector Labs, SK-4105; Burlingame, CA) was used, with DAB chromagen applied for 40-45 seconds.

IHC images were taken and scanned on an Aperio AT2 instrument by the University of Michigan Pathology departmental Slide Scanning Service at 40X (Figure 1A, B top panel, c^1, c^2, and D; Figure 3A) and on an IHC Olympus SZX16 at 8x zoom (Figure 1B bottom panel). 100X insets were captured on a Zeiss Axio M1 (Figure $1a^2$). Brightfield images were captured on an Olympus IX70, with a DP71 digital camera (Figure 4A, C).

LGR5 Immunohistochemistry scoring for staining intensity in the epithelium and in the stroma

The TMA, along with 5 additional FFPE normal colon samples from autopsies, were scored for staining intensity in both the epithelium and then separately in the stroma (Figure 3). Two FFPE biopsied

bioRxiv preprint doi: https://doi.org/10.1101/118034; this version posted March 18, 2017. The copyright holder for this preprint (which was not certified by peer review) is the author/funder, who has granted bioRxiv a license to display the preprint in perpetuity. It is made available under aCC-BY 4.0 International license.

large (> 10mm) adenomas, used to derive organoids for this study, were also assessed for reactivity (specimen 282 and 590), but these were not simultaneously scored since they were stained under different conditions (Figure 4C left column). Scoring was conducted by two independent viewers on blinded samples at 8X and 20X magnification. Scoring key: 0 = non-specific or < 1%; 1 = 1-10% or only evident at 20X magnification; 2 = 10-50% or light diffuse staining >50%; 5 = >50%. A standard pathology peer review method was used to resolve discrepancies in scoring between two independent scorers, with a third party reviewer intervening when necessary (Morton et al. 2010). The vast majority of samples were in concordance between the two viewers. Stage T2 (n=25) and T3 (n=44) tumors were compared to normal colon and adenoma (termed Stage T0; n=10). TMA cancers with grades I and I-II were grouped (termed "Grade I"; n=20) and cancers grade II-III and III were grouped (termed "Grade III"; n=10) for further analyses. LGR5 stromal and epithelial staining for adenomas (n=3), and Grade I, II (n=38), and III cancers were compared to normal colon tissue (n=7). Differences in LGR5 staining in the stroma or epithelium by stage or grade were quantified by linear regression.

LGR5 Immunofluorescence

Rehydrated sections were retrieved with R-Buffer B (pH 8.5; Electron Microscopy Sciences) in a pressurized Retriever 2100 (Electron Microscopy Sciences) overnight. After 3X PBS washing, slides were blocked for 1 hour with 0.5% Triton X-100 and 5% donkey serum in PBS. Slides were incubated overnight at 4°C with the following antibodies in 0.05% Tween 20 and 5% donkey serum: LGR5 clone 89.11 at 1:500 (Figure 1c[3]c[4]); anti-OLFM4 antibody at 1:500 (Abcam, #ab85046; Cambridge, MA)(Figure 8C); anti-defensin5a at 1:500 (Abcam, #ab90802)(Figure 2A); anti-E-cadherin at 1:500 (BD Biosciences, # 610181, San Jose, CA) (Figure 8C); and anti-E-cadherin at 1:500 (R&D, #AF748)(Figure 2A). Slides were washed 3X for 5 minutes each, followed by 1 hour room temperature incubation with the following secondaries (1:1000): LGR5 plus DAPI (Figure 1c[3]/c[4]; Figure 2A) and OLFM4 (Figure 8C) secondaries (biotinylated secondary donkey anti-rabbit; Jackson Immuno Research Labs, #711-065-152; West Grove, PA); defensin5a (Figure 2A) and E-cadherin secondary (Figure 8C)(donkey anti-mouse 488; Jackson Immuno Research Labs, #715-545-150); E-cadherin secondary (Figure 2A) (donkey anti-goat 647; Jackson Immuno Research Labs,

bioRxiv preprint doi: https://doi.org/10.1101/118034; this version posted March 18, 2017. The copyright holder for this preprint (which was not certified by peer review) is the author/funder, who has granted bioRxiv a license to display the preprint in perpetuity. It is made available under aCC-BY 4.0 International license.

#705-605-147). Slides were washed 3X. LGR5 and OLFM4 were amplified with the SK4105 TSA Kit with Alexa 594 tyramide (Invitrogen, #T20935). All slides were mounted with Prolong Gold without DAPI (Molecular Probes, #P36930). Images were taken on a Nikon A1 confocal microscope.

LGR5 in Situ Hybridization

Formalin fixed, paraffin sections were cut at 5-6 microns and rehydrated to water. *In situ* hybridization was performed using the RNAscope 2.0 HD detection kit [Advanced Cell Diagnostics (ADC), #310035; Newark, CA] according to the standard provided protocol (Figure 1B, D). The human LGR5 probe was designed by ADC using the NCBI LGR5 sequence (NCBI Reference Sequence: NM_003667.2) and targets the region between 560-1589 base pairs (HS-LGR5, 311021, lot 15022A). All incubations were performed at 40°C in the ADC HybEZ hybridization system oven (#310010). Images were taken and scanned on an Aperio AT2 instrument by the University of Michigan Pathology departmental Slide Scanning Service.

Single Cell Isolation and by Magnetic-Activated Cell Sorting for LGR5(+) and LGR5(-) cells (Figure 4)

<u>Organoid dissociation into single cells</u>

On the day of sorting, the cultures were treated with 10µM Y27632 for 2.5 hrs prior to harvest. Matrigel was digested for 45 minutes with cold 2mM EDTA in DPBS and organoids were washed 3X with cold DPBS (100xg at 4℃). Structures were dissociated into single cells using the Tumor Dissociation Kit (human) (Miltenyi Biotec, #130-095-929) with the protocol modifications described as follows. The enzymes were prepared in warm HBSS modified to 0.13mM calcium and 0.9mM magnesium [10% HBSS, calcium, magnesium, no phenol red (Gibco, #14025092) with 90% HBSS, no calcium, no magnesium (Gibco, #14170112)] to minimize differentiation of the epithelial cells while supporting enzymatic activity. The organoids were suspended in 20mL of enzyme solution containing 5µM Y27632, then transferred to two BSA-coated C-tubes (Miltenyi Biotec, #130-096-334) and dissociated with a gentleMACS Dissociator (Miltenyi Biotec, #130-093-235) using the program *h_tumor_01*, once at the onset and every 15 minutes for 1 hour, and finishing with two program runs. Between runs the suspension was slowly rotated at 37°C. The

bioRxiv preprint doi: https://doi.org/10.1101/118034; this version posted March 18, 2017. The copyright holder for this preprint (which was not certified by peer review) is the author/funder, who has granted bioRxiv a license to display the preprint in perpetuity. It is made available under aCC-BY 4.0 International license.

cell suspension was then poured over a succession of cold BSA-coated cell strainers into 0.5% BSA-2mM EDTA-PBS: 100µm (Corning, #DL 352360) to 40µm (Corning, #DL 352340) to 20µm (CellTrics of Sysmex Europe GmbH, #04-0042-2315; Norderstedt, Germany). The cells were washed 3X in the 0.5% BSA-2mM EDTA-PBS and centrifuged for 5 minutes at 500xg. Cells were counted under trypan blue exclusion to estimate live cell number using a Countess Automated Cell Counter (Invitrogen, #C10227).

Magnetic bead-LGR5 antibody labeling

Single cells were resuspended and processed in cold 0.5% BSA-2mM EDTA-PBS containing 5µM Y27632 in a BSA-coated tube (using BSA-coated tips for mixing) pelleted at 500xg, and otherwise stained according to the product instructions (Miltenyi Biotec: Anti-human LGR5 MicroBeads #130-104-072; clone 22H2.8; APC-Check Reagent #130-098-892).

Magnetic separation

Stained cells were resuspended at 10^7 cells/mL in a DNAse Buffer containing HBSS (1:10 $Ca^{2+}Mg^{2+}$), 0.5% BSA, 5µM Y27632, 200 Kunitz units/mL DNAse (Sigma-Aldrich, #D5025). Cells were applied over the columns (Miltenyi Biotec, LS Columns , # 130-042-401) through a cold BSA-coated 20µm cell strainer at 1mL per column. Columns were prepped by coating in the DNAse Buffer for 45 minutes at 4°C prior to use. All washes were performed with the DNAse Buffer. After removing the column from the magnet, 2mL DNAse Buffer was applied to the column to flush out the magnetically-bound cells into a 15mL BSA-coated tube. Unlabeled flow-through cells (magnet intact) and labeled magnet-bound cells were pelleted at 500xg for 5 minutes and resuspended in 0.1% BSA-PBS-2mM EDTA with 10µM Y27632.

Flow Cytometry

Cells were analyzed on a LSRII cytometer (BD Biosciences) and sorted on a MoFlo Astrios (Beckman Coulter; Brea, California) instrument at the University of Michigan Cancer Center Flow Cytometry core facility. Events first passed through a routine light-scatter and doublet discrimination gate, followed by exclusion of dead cells using 4',6-diamidino-2-phenylindole (1µM DAPI dilactate; Molecular Probes, # D3571). Gating strategy set the APC-positive cell population at 0.05-0.1% of the viable MACS

bioRxiv preprint doi: https://doi.org/10.1101/118034; this version posted March 18, 2017. The copyright holder for this preprint (which was not certified by peer review) is the author/funder, who has granted bioRxiv a license to display the preprint in perpetuity. It is made available under aCC-BY 4.0 International license.

flow-through cells, LGR5(FT+) (Figure 4D; Figure S1A; Figure 8A, specimen 81, 83). Gating strategy set the APC-positive cell population at 0.05-0.1% of the viable FMO-APC check reagent control for the analysis of samples that were not MACS processed (Figure 4D top and middle rows; Figure S1A). For RNA expression analyses, cell fractions were sorted into RLT lysis buffer (Qiagen). Flow cytometric data analysis was performed using Winlist 3D software (Verity) and FlowJo vX.0.7 (Tree Star). For each specimen, three cell fractions were FACS and collected (Figure 4A; Figure S2): MACS magnet-bound positives, LGR5(+); MACS magnet-bound negatives, LGR5(-); and MACS unbound flow-through, LGR5(FT-).

Normal Colinic Crypt Isolation from Tissue, Single Cell Dissociation, Magnetic Separation and Flow Cytometry

Crypts were isolated from three warm autopsy normal colon specimens (6 cm^2) and processed as previously described (Dame et al. 2014), a modification of Sato et al (Sato, Stange, et al. 2011). Crypts were dissociated into single cells, as described above for the adenoma organoids, and a final 1mL of a dense crypt pellet was processed per C-tube. Magnetic separation and flow cytometry (Becton-Dickinson FACSAria III sorter) were as above, with the added gating/analysis for EpCAM expression using a phycoerythrin (PE)-conjugated antibody (2µg /mL buffer/$\leq 10^6$ cells; BioLegend, #324205; San Diego, CA) and an EpCAM isotype control (2µg /mL buffer/$\leq 10^6$ cells; BioLegend, #400311). EpCAM-PE(+)/DAPI(-) cells were interrogated for LGR5 expression as done above with MAC processed samples (Figure 8A, specimen 81,83) or with rigorous so-called fluorescence-minus-one controls [FMO; DAPI(-), EpCAM(+)] for sorting of pre-magnet cells (Figure 8A, specimen 84).

High Throughput RNA Sequencing (RNA-seq)

RNA was extracted from sorted cells using the RNeasy Micro Kit (Qiagen, #74004) with on column DNase digestion. RNA concentration and quality were determined using a Nanodrop (Thermo Scientific) and Bioanalyzer (Agilent). Due to the small number of cells following FACS and corresponding low level of input RNA, we depleted ribosomal RNAs with RiboGone (Takara Clontech, #634846; Mountain View, CA) and prepared sequencing libraries utilizing the SMARTer Stranded RNA-Seq kit (Takara Clontech, #

bioRxiv preprint doi: https://doi.org/10.1101/118034; this version posted March 18, 2017. The copyright holder for this preprint (which was not certified by peer review) is the author/funder, who has granted bioRxiv a license to display the preprint in perpetuity. It is made available under aCC-BY 4.0 International license.

634839) following the manufacturer's recommended protocol. Libraries were multiplexed over 2 lanes and sequenced using paired end 75 cycle reads (sample 14881) and 125 cycle reads (samples 282, 584, and 590) on a HiSeq sequencer (Illumina) at the University of Michigan DNA Sequencing Core Facility (Figure 5; Figure S2).

RNA-Seq Data Analysis

Alignment and quality control

Computational analyses were performed using the Flux high-performance computer cluster hosted by Advanced Research Computing (ARC) at the University of Michigan. Raw sequencing read quality was assessed utilizing FastQC. The first five nucleotides of the both reads in each read pair were trimmed with SeqTK due to the presence of adapter sequence and high nucleotide redundancy. A splice junction aware build of the human genome (GRCh37) was built using the genomeGenerate function from STAR 2.3.0 (Dobin et al. 2013). Read pairs were aligned to the genome using STAR, using the options "outFilterMultimapNmax 10" and "sjdbScore 2".

Differential expression testing

The aligned reads were assigned to genomic features (GRCh37 genes) using HTSeq-count, with the set mode "union". We conducted differential expression testing on the assigned read counts per gene utilizing edgeR (Robinson, McCarthy, and Smyth 2010). Analysis were conducted to compare expression of LGR5(+), LGR5(-), and LGR5(FT-) cells, adjusting for study subject as a covariate using glmLRT. To reduce the dispersion of the dataset due to lowly expressed genes, genes with a mean aligned read count less than five across all samples were excluded from analysis. Normalized counts per million were estimated utilizing the "cpm" function in edgeR. Genes were considered differentially expressed between conditions at a false discovery rate adjusted p-value < 0.05 (Figure 5; Figure S2; Table S1).(Benjamini and Hochberg 1995).

bioRxiv preprint doi: https://doi.org/10.1101/118034; this version posted March 18, 2017. The copyright holder for this preprint (which was not certified by peer review) is the author/funder, who has granted bioRxiv a license to display the preprint in perpetuity. It is made available under aCC-BY 4.0 International license.

Comparison to previously published datasets

RNA-seq data from normal colon (samples ERR315348, ERR315357, ERR315400, ERR315403, ERR315462, ERR315484 from Tissue Based Map of the Human Proteome Science REF) were processed as described above, and differential gene expression between the LGR5(+) cells and normal colon were calculated as described above (Figure 6C, D). Overlap between genes overexpressed in LGR5(+) cells with the previously reported *Lgr5*+ ISC gene signature (Munoz et al. 2012) was calculated by identifying the overlap between genes present in both the Muñoz et al ISC gene expression signature and genes identified as upregulated in LGR5(+) adenoma cells (Figure 6B; Table S2). Statistical significance of the overlap between these gene signatures was calculated using the hypergeometric distribution. Genes in the Muñoz et al ISC signature that were not present at detectable levels in our dataset were excluded from this calculation.

Pathway analyses

Differentially expressed pathways were identified utilizing iPathways (Advaita; Plymouth, MI). A directional analysis was conducted on all genes by including *P*-value of the differential expression test as a measure of effect size and log2 fold difference in expression as a measure of effect direction. KEGG biological pathways and Gene Ontology biological processes were considered differentially expressed at a *P*-value <0.05 (Figure S3-8; Table S1).

DKK4 (Dickkopf WNT Signaling Pathway Inhibitor-4) Interrogation; Comparisons to LGR5 Expression.

DKK4 and *LGR5* quantitative real-time PCR of adenoma organoids grown in L-WRN vs. KGMG

Cultured organoids from three adenomas, 282, 584, and 590, were transitioned from KGMG to L-WRN, with the concomitant shift from budding to cystic structures. *LGR5* and *DKK4* mRNA expression were then assessed as previously described above and presented as increased expression in L-WRN relative to KGMG (Figure 7A). DKK4 primer sequences were as follows: *hDKK4* (Cui, Taub, and Gardner 2007): GGAGCTCTGGTCCTGGACTT (Forward primer); TCTGGTATTGCAGTCCGTGT (Reverse primer); 102 bp band size.

bioRxiv preprint doi: https://doi.org/10.1101/118034; this version posted March 18, 2017. The copyright holder for this preprint (which was not certified by peer review) is the author/funder, who has granted bioRxiv a license to display the preprint in perpetuity. It is made available under aCC-BY 4.0 International license.

Recombinant human DKK4 protein treatment of adenoma organoids

Three organoid specimens (282, 584, 590) were prepared for treatment as previously described (Xue et al.). Organoids were removed from Matrigel and mechanically dissociated into uniform structures between 20-100 µm in diameter with the gentleMACS (Miltenyi Biotec) using programs *h_Tumor_01.01* followed by *m_Lung_01.01*, and then by passing through a BSA-coated 100µm cell strainer. Organoids were then seeded at 1:1 split ratio at approximately 3000 small organoids/50 µl Matrigel pad/well/24-well plates. After 24 hrs of plating, the cultures were treated with 0.5 and 4.0µg/mL (350µL/well) of recombinant DKK4 (R&D Systems, #1269-DK) for 72 hrs in either KGMG or L-WRN. Treated organoids were harvested and assessed for changes in LGR5 mRNA by qPCR (Figure S10C).

DKK4 knockdown organoids

Stable adenoma organoid *DKK4* knockdowns and scramble small hairpin RNA were generated with lentivirus infection of adenoma organoid specimen 282 and selected with 1µg/mL puromycin (Xue et al.). The GIPZ lentiviral shRNA vectors (Open Biosystems of GE Dharmacon; Lafayette, CO) for human *DKK4* sh1DKK4 (Clone ID: V2LHS_204025) and sh2DKK4 (Clone ID: V2LHS_197942) have bicistronic expression of GFP and the puromycin selection marker to allow visualized by GFP fluorescence. To assess transduction efficiency, and the effect of *DKK4* knockdown on *LGR5*, knockdowns grown in both KGMG and L-WRN were analyzed for changes in mRNA by qPCR (Figure 7D).

bioRxiv preprint doi: https://doi.org/10.1101/118034; this version posted March 18, 2017. The copyright holder for this preprint (which was not certified by peer review) is the author/funder, who has granted bioRxiv a license to display the preprint in perpetuity. It is made available under aCC-BY 4.0 International license.

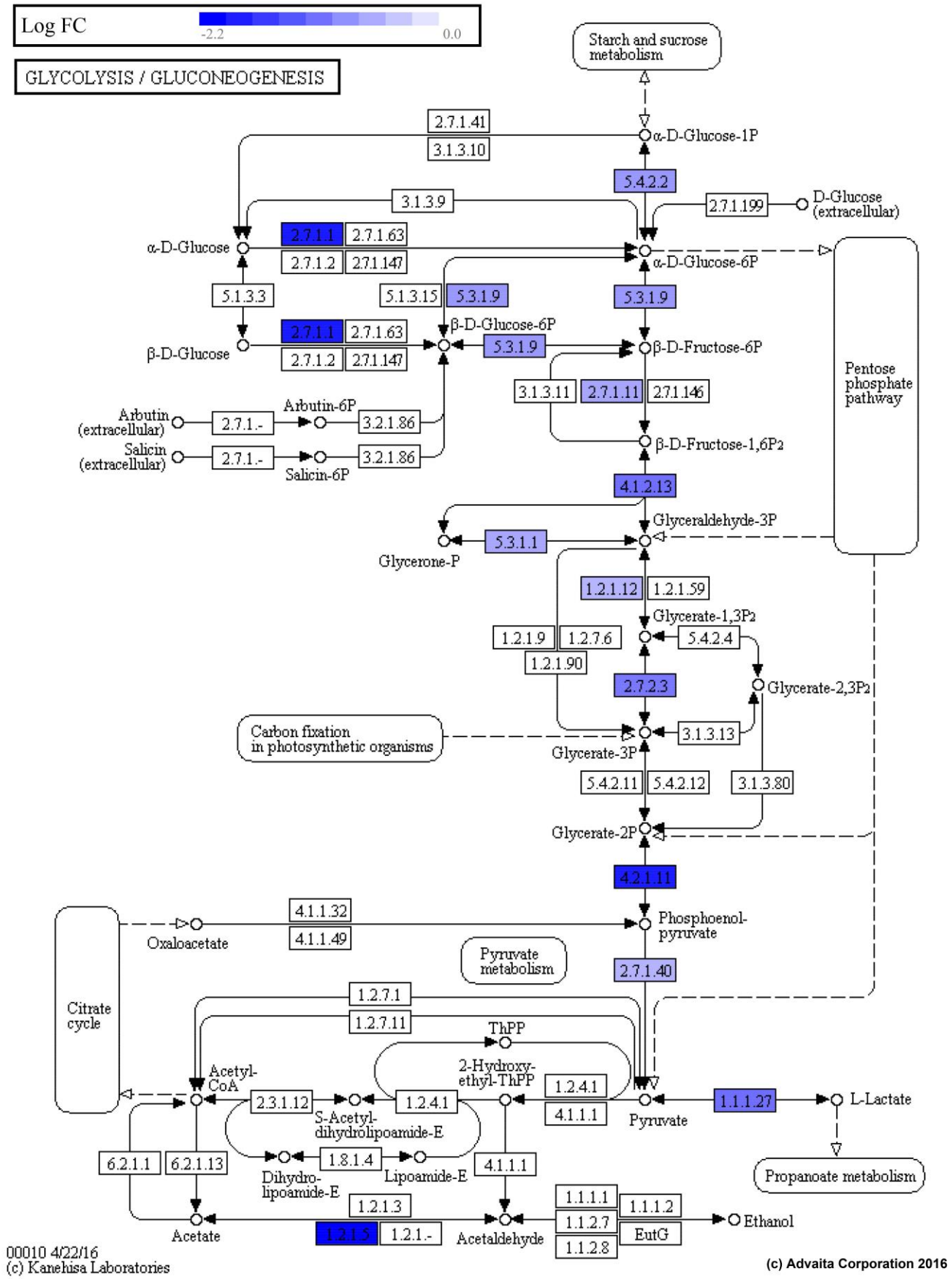

Figure S3 (Related to Figure 5): Relative expression of genes involved in the KEGG pathway "Glycolysis and Gluconeogenesis" between LGR5(+) and LGR5(-) human adenoma cells (*P*-value=6.57E-09).

bioRxiv preprint doi: https://doi.org/10.1101/118034; this version posted March 18, 2017. The copyright holder for this preprint (which was not certified by peer review) is the author/funder, who has granted bioRxiv a license to display the preprint in perpetuity. It is made available under aCC-BY 4.0 International license.

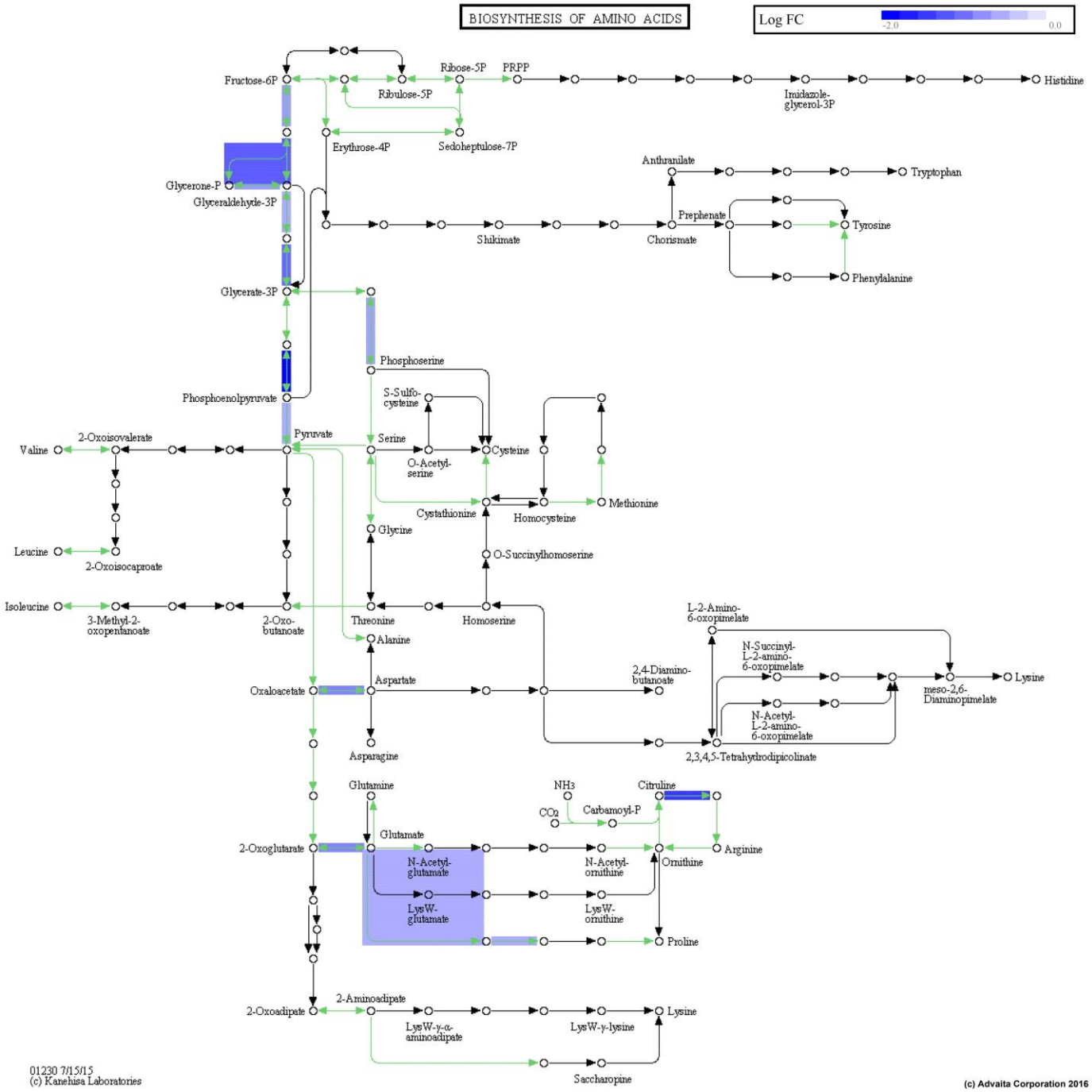

Figure S4 (Related to Figure 5): Relative expression of genes involved in the KEGG pathway "Biosynthesis of Amino Acids Pathway" between LGR5(+) and LGR5(-) human adenoma cells (*P*-value=4.32E-07).

bioRxiv preprint doi: https://doi.org/10.1101/118034; this version posted March 18, 2017. The copyright holder for this preprint (which was not certified by peer review) is the author/funder, who has granted bioRxiv a license to display the preprint in perpetuity. It is made available under aCC-BY 4.0 International license.

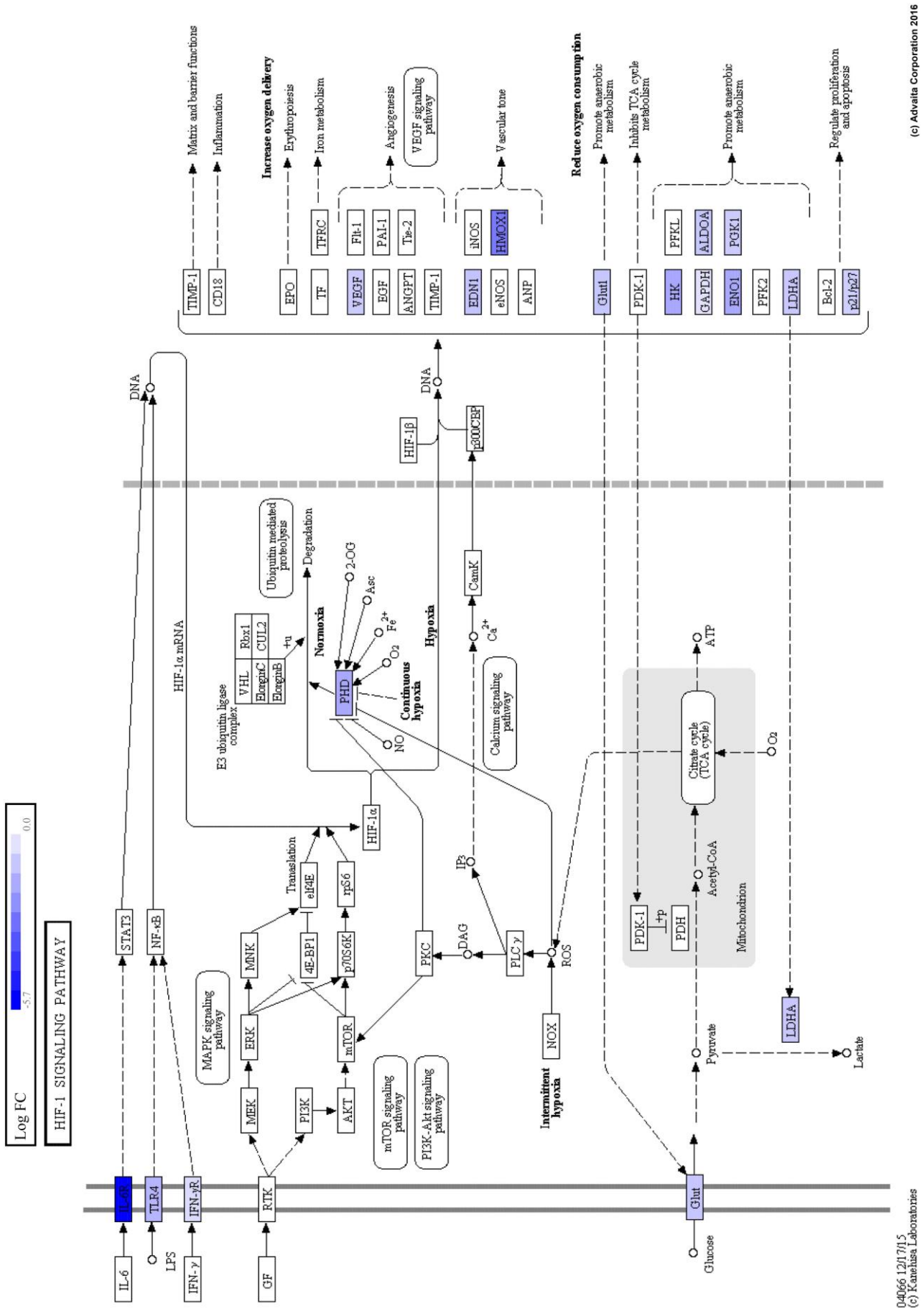

Figure S5 (Related to Figure 5): Relative expression of genes involved in the KEGG pathway "HIF-1 Signaling Pathway" between LGR5(+) and LGR5(-) human adenoma cells (*P*-value=1.42E-05).

bioRxiv preprint doi: https://doi.org/10.1101/118034; this version posted March 18, 2017. The copyright holder for this preprint (which was not certified by peer review) is the author/funder, who has granted bioRxiv a license to display the preprint in perpetuity. It is made available under aCC-BY 4.0 International license.

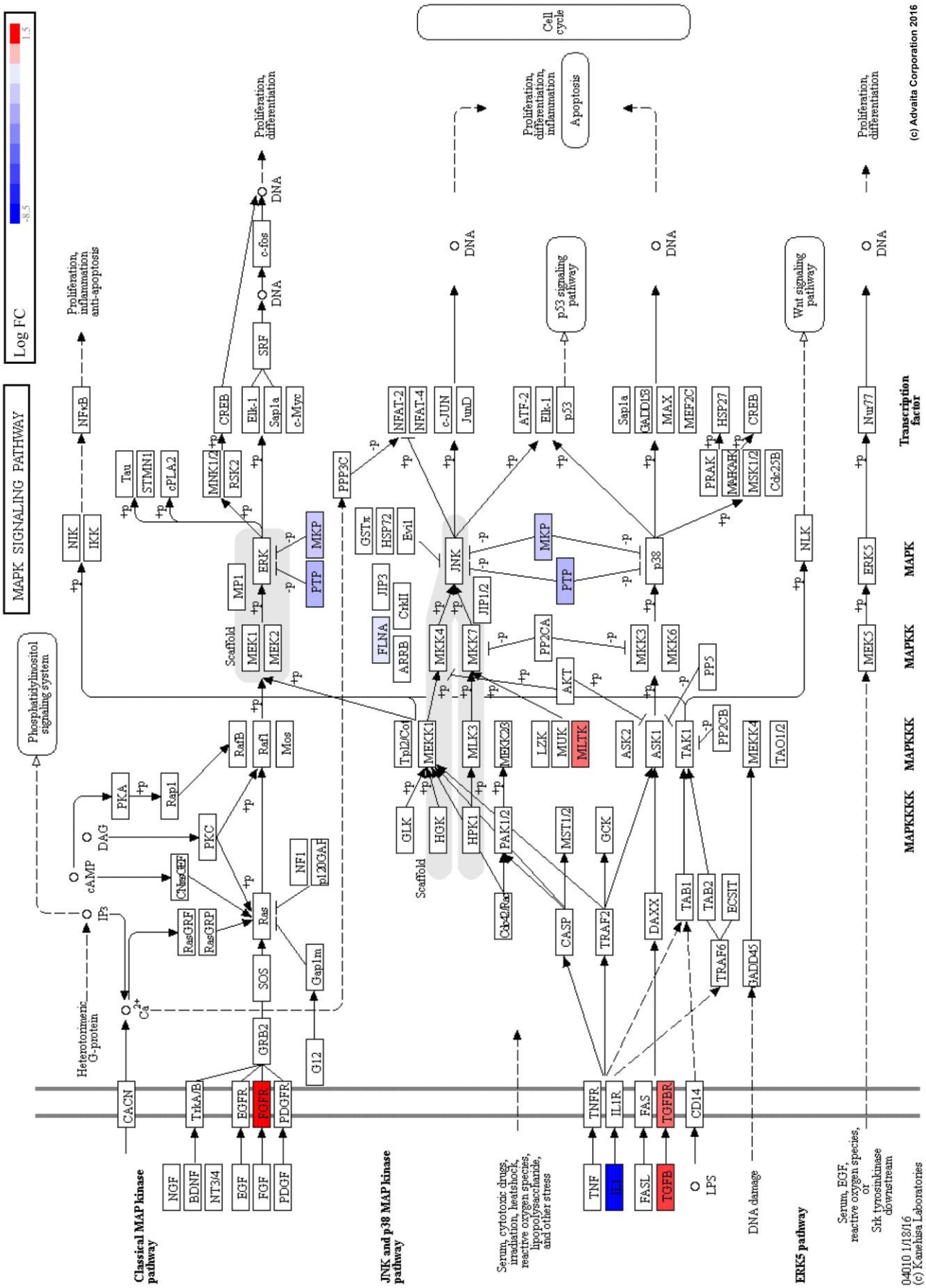

Figure S6 (Related to Figure 5): Relative expression of genes involved in the KEGG pathway "MAPK Signaling Pathway" between LGR5(+) and LGR5(-) human adenoma cells (*P*-value=.0105).

bioRxiv preprint doi: https://doi.org/10.1101/118034; this version posted March 18, 2017. The copyright holder for this preprint (which was not certified by peer review) is the author/funder, who has granted bioRxiv a license to display the preprint in perpetuity. It is made available under aCC-BY 4.0 International license.

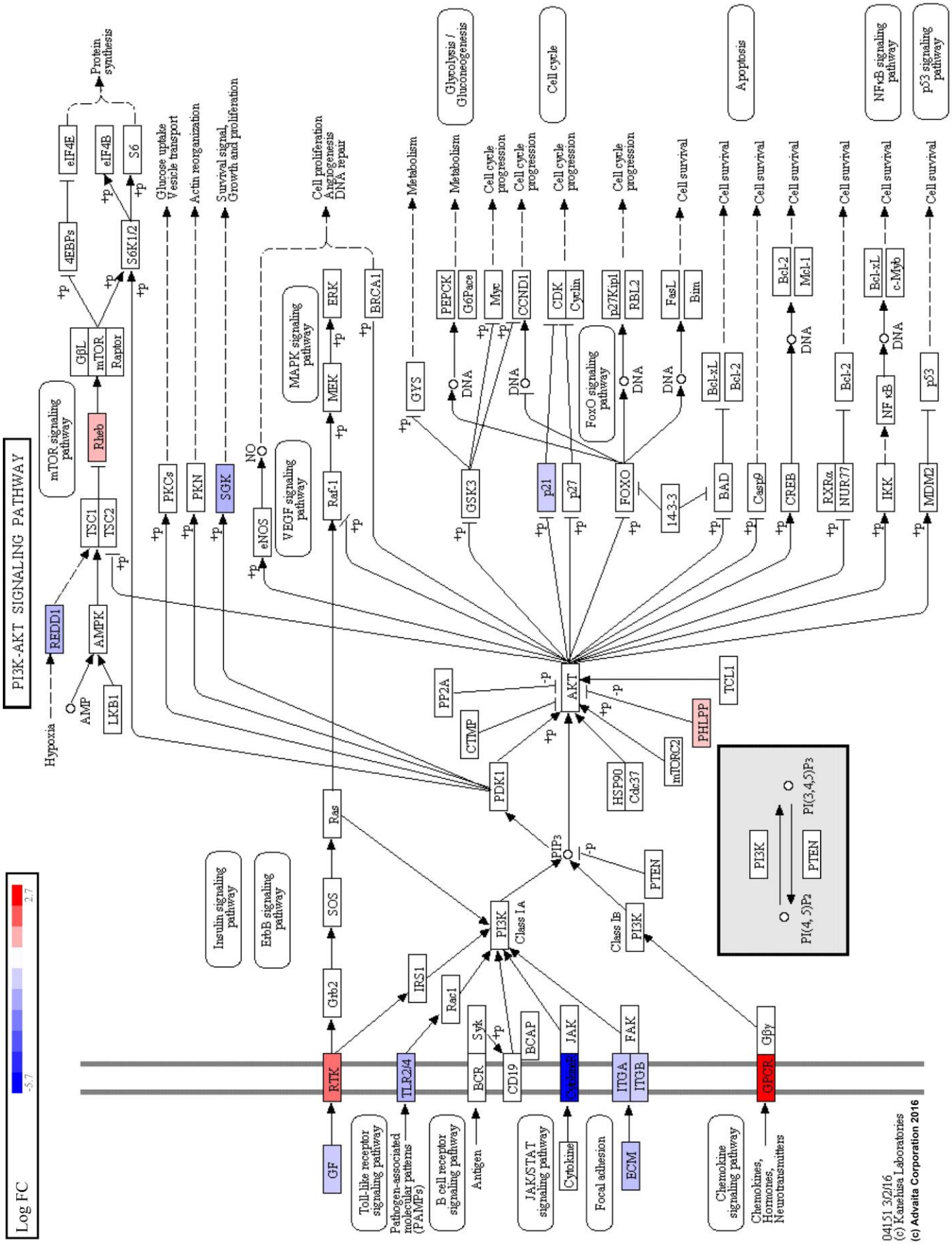

Figure S7 (Related to Figures 5): Relative expression of genes involved in the KEGG pathway "PI3K AKT Signaling Pathway" between LGR5(+) and LGR5(-) human adenoma cells (*P*-value=.0102).

bioRxiv preprint doi: https://doi.org/10.1101/118034; this version posted March 18, 2017. The copyright holder for this preprint (which was not certified by peer review) is the author/funder, who has granted bioRxiv a license to display the preprint in perpetuity. It is made available under aCC-BY 4.0 International license.

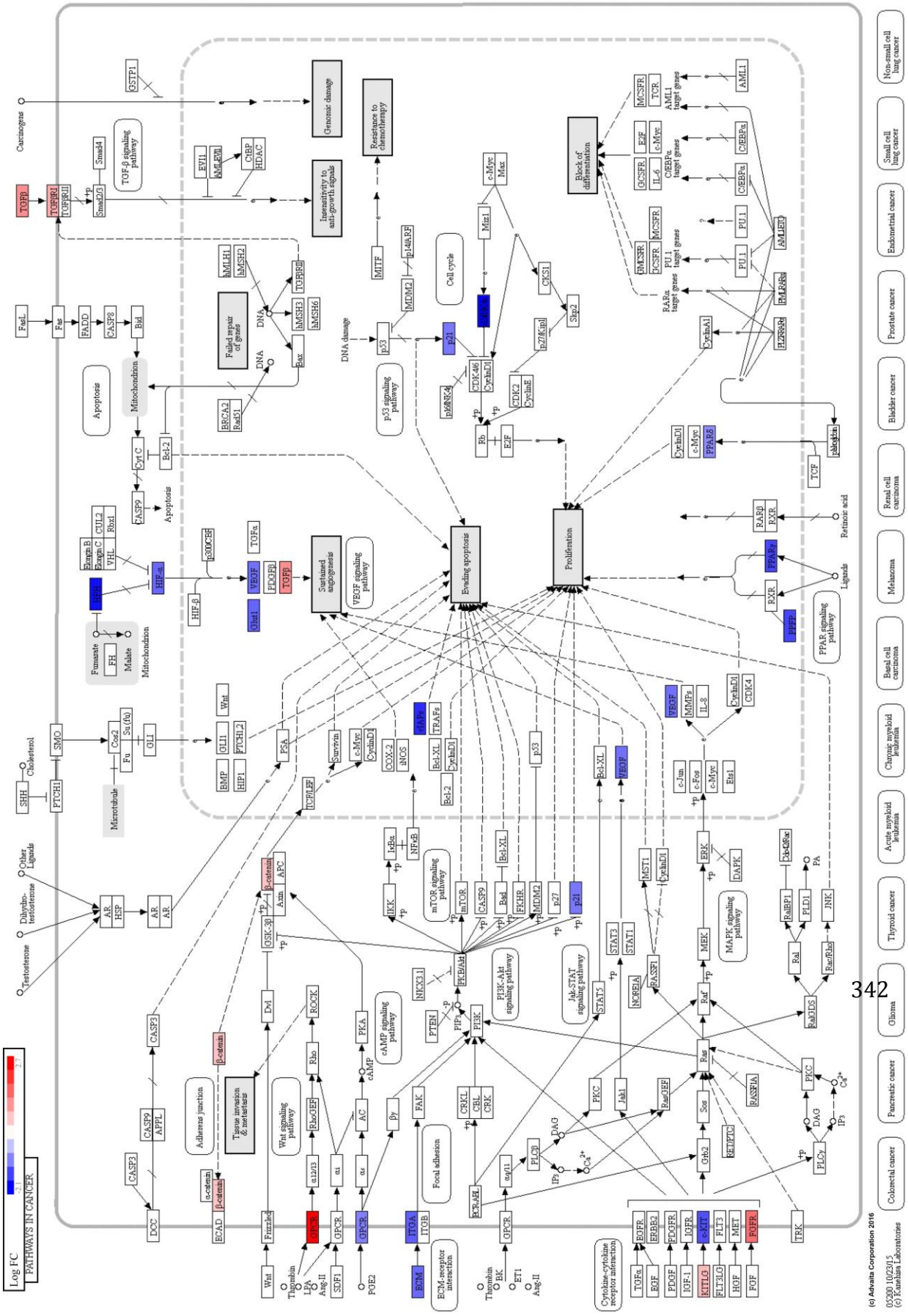

Figure S8 (Related to Figure 5): Relative expression of genes involved in the KEGG pathway "Pathways in Cancer" between LGR5(+) and LGR5(-) human adenoma cells (*P*-value=.0133)

bioRxiv preprint doi: https://doi.org/10.1101/118034; this version posted March 18, 2017. The copyright holder for this preprint (which was not certified by peer review) is the author/funder, who has granted bioRxiv a license to display the preprint in perpetuity. It is made available under aCC-BY 4.0 International license.

Table S1 (Related to Figure 5, Figure 6 and Figure S2-8): LGR5(+) Adenoma RNA-seq analyses

Tab 1: LGR5(+) vs. LGR5(-) significant genes

Tab 2: LGR5(+) vs. LGR5(-) all genes

Tab 3: LGR5(+) vs. LGR5(FT-) significant genes

Tab 4: LGR5(+) vs. LGR5(FT-) all genes

Tab 5: LGR5(+) gene signature

Tab 6: LGR5(+) vs. LGR5(-) significant KEGG pathways

Tab 7: LGR5(+) vs. LGR5(FT-) significant KEGG pathways

Tab 8: LGR5(+) adenoma cell vs. normal colon gene expression for genes in the "LGR5+ adenoma stem cell gene expression signature"

bioRxiv preprint doi: https://doi.org/10.1101/118034; this version posted March 18, 2017. The copyright holder for this preprint (which was not certified by peer review) is the author/funder, who has granted bioRxiv a license to display the preprint in perpetuity. It is made available under aCC-BY 4.0 International license.

Supplemental References

"Database of Single Nucleotide Polymorphisms (dbSNP). Bethesda (MD): National Center for Biotechnology Information, National Library of Medicine. (dbSNP Build ID: 138). http://www.ncbi.nlm.nih.gov/SNP/."

Abecasis, G. R., A. Auton, L. D. Brooks, M. A. DePristo, R. M. Durbin, R. E. Handsaker, H. M. Kang, G. T. Marth, and G. A. McVean. 2012. "An integrated map of genetic variation from 1,092 human genomes." *Nature* no. 491 (7422):56-65. doi: 10.1038/nature11632.

Benjamini, Yoav, and Yosef Hochberg. 1995. "Controlling the False Discovery Rate: A Practical and Powerful Approach to Multiple Testing." *Journal of the Royal Statistical Society. Series B (Methodological)* no. 57 (1):289-300. doi: citeulike-article-id:1042553 doi: 10.2307/2346101.

Cibulskis, K., M. S. Lawrence, S. L. Carter, A. Sivachenko, D. Jaffe, C. Sougnez, S. Gabriel, M. Meyerson, E. S. Lander, and G. Getz. 2013. "Sensitive detection of somatic point mutations in impure and heterogeneous cancer samples." *Nat Biotechnol* no. 31 (3):213-9. doi: 10.1038/nbt.2514.

Cingolani, P., A. Platts, L. Wang le, M. Coon, T. Nguyen, L. Wang, S. J. Land, X. Lu, and D. M. Ruden. 2012. "A program for annotating and predicting the effects of single nucleotide polymorphisms, SnpEff: SNPs in the genome of Drosophila melanogaster strain w1118; iso-2; iso-3." *Fly (Austin)* no. 6 (2):80-92. doi: 10.4161/fly.19695.

Cui, W., D. D. Taub, and K. Gardner. 2007. "qPrimerDepot: a primer database for quantitative real time PCR." *Nucleic Acids Res* no. 35 (Database issue):D805-9. doi: 10.1093/nar/gkl767.

Dame, Michael K., Yan Jiang, Henry D. Appelman, Kelly D. Copley, Shannon D. McClintock, Muhammad Nadeem Aslam, Durga Attili, B. Joseph Elmunzer, Dean E. Brenner, James Varani, and D. Kim Turgeon. 2014. "Human colonic crypts in culture: segregation of immunochemical markers in normal versus adenoma-derived." *Lab Invest* no. 94 (2):222-234. doi: 10.1038/labinvest.2013.145.

DePristo, M. A., E. Banks, R. Poplin, K. V. Garimella, J. R. Maguire, C. Hartl, A. A. Philippakis, G. del Angel, M. A. Rivas, M. Hanna, A. McKenna, T. J. Fennell, A. M. Kernytsky, A. Y. Sivachenko, K. Cibulskis, S. B. Gabriel, D. Altshuler, and M. J. Daly. 2011. "A framework for variation discovery and genotyping using next-generation DNA sequencing data." *Nat Genet* no. 43 (5):491-8. doi: 10.1038/ng.806.

Dobin, A., C. A. Davis, F. Schlesinger, J. Drenkow, C. Zaleski, S. Jha, P. Batut, M. Chaisson, and T. R. Gingeras. 2013. "STAR: ultrafast universal RNA-seq aligner." *Bioinformatics* no. 29 (1):15-21. doi: 10.1093/bioinformatics/bts635.

Drost, J., R. H. van Jaarsveld, B. Ponsioen, C. Zimberlin, R. van Boxtel, A. Buijs, N. Sachs, R. M. Overmeer, G. J. Offerhaus, H. Begthel, J. Korving, M. van de Wetering, G. Schwank, M. Logtenberg, E. Cuppen, H. J. Snippert, J. P. Medema, G. J. Kops, and H. Clevers. 2015. "Sequential cancer mutations in cultured human intestinal stem cells." *Nature* no. 521 (7550):43-7. doi: 10.1038/nature14415.

Farin, H. F., J. H. Van Es, and H. Clevers. 2012. "Redundant sources of Wnt regulate intestinal stem cells and promote formation of Paneth cells." *Gastroenterology* no. 143 (6):1518-1529 e7. doi: 10.1053/j.gastro.2012.08.031.

Finkbeiner, S. R., and J. R. Spence. 2013. "A gutsy task: generating intestinal tissue from human pluripotent stem cells." *Dig Dis Sci* no. 58 (5):1176-84. doi: 10.1007/s10620-013-2620-2.

Fujii, M., M. Shimokawa, S. Date, A. Takano, M. Matano, K. Nanki, Y. Ohta, K. Toshimitsu, Y. Nakazato, K. Kawasaki, T. Uraoka, T. Watanabe, T. Kanai, and T. Sato. 2016. "A Colorectal Tumor Organoid Library Demonstrates Progressive Loss of Niche Factor Requirements during Tumorigenesis." *Cell Stem Cell* no. 18 (6):827-38. doi: 10.1016/j.stem.2016.04.003.

bioRxiv preprint doi: https://doi.org/10.1101/118034; this version posted March 18, 2017. The copyright holder for this preprint (which was not certified by peer review) is the author/funder, who has granted bioRxiv a license to display the preprint in perpetuity. It is made available under aCC-BY 4.0 International license.

Gates, Chris, Jessica Bene, Ashwini Bhasi, Peter J. Ulintz, Kevin Meng, and James Cavalcoli. 2015. "Jacquard: A practical approach to integrating complex somatic variant data sets. https://github.com/umich-brcf-bioinf/Jacquard."

Koboldt, D. C., Q. Zhang, D. E. Larson, D. Shen, M. D. McLellan, L. Lin, C. A. Miller, E. R. Mardis, L. Ding, and R. K. Wilson. 2012. "VarScan 2: somatic mutation and copy number alteration discovery in cancer by exome sequencing." *Genome Res* no. 22 (3):568-76. doi: 10.1101/gr.129684.111.

Li, H., and R. Durbin. 2009. "Fast and accurate short read alignment with Burrows-Wheeler transform." *Bioinformatics* no. 25 (14):1754-60. doi: 10.1093/bioinformatics/btp324.

Liu, X., X. Jian, and E. Boerwinkle. 2011. "dbNSFP: a lightweight database of human nonsynonymous SNPs and their functional predictions." *Hum Mutat* no. 32 (8):894-9. doi: 10.1002/humu.21517.

Liu, X., X. Jian, and E. Boerwinkle. 2013. "dbNSFP v2.0: a database of human non-synonymous SNVs and their functional predictions and annotations." *Hum Mutat* no. 34 (9):E2393-402. doi: 10.1002/humu.22376.

Matano, M., S. Date, M. Shimokawa, A. Takano, M. Fujii, Y. Ohta, T. Watanabe, T. Kanai, and T. Sato. 2015. "Modeling colorectal cancer using CRISPR-Cas9-mediated engineering of human intestinal organoids." *Nat Med* no. 21 (3):256-62. doi: 10.1038/nm.3802.

Miyoshi, Hiroyuki, and Thaddeus S. Stappenbeck. 2013. "In vitro expansion and genetic modification of gastrointestinal stem cells in spheroid culture." *Nat. Protocols* no. 8 (12):2471-2482. doi: 10.1038/nprot.2013.153
http://www.nature.com/nprot/journal/v8/n12/abs/nprot.2013.153.html#supplementary-information.

Morton, Daniel, Rani S. Sellers, Erio Barale-Thomas, Brad Bolon, Catherine George, Jerry F. Hardisty, Armando Irizarry, Jennifer S. McKay, Marielle Odin, and Munehiro Teranishi. 2010. "Recommendations for Pathology Peer Review." *Toxicologic Pathology* no. 38 (7):1118-1127. doi: 10.1177/0192623310383991.

Munoz, J., D. E. Stange, A. G. Schepers, M. van de Wetering, B. K. Koo, S. Itzkovitz, R. Volckmann, K. S. Kung, J. Koster, S. Radulescu, K. Myant, R. Versteeg, O. J. Sansom, J. H. van Es, N. Barker, A. van Oudenaarden, S. Mohammed, A. J. Heck, and H. Clevers. 2012. "The Lgr5 intestinal stem cell signature: robust expression of proposed quiescent '+4' cell markers." *EMBO J* no. 31 (14):3079-91. doi: 10.1038/emboj.2012.166

Onuma, K., M. Ochiai, K. Orihashi, M. Takahashi, T. Imai, H. Nakagama, and Y. Hippo. 2013. "Genetic reconstitution of tumorigenesis in primary intestinal cells." *Proc Natl Acad Sci U S A* no. 110 (27):11127-32. doi: 10.1073/pnas.1221926110.

Quinlan, A. R., and I. M. Hall. 2010. "BEDTools: a flexible suite of utilities for comparing genomic features." *Bioinformatics* no. 26 (6):841-2. doi: 10.1093/bioinformatics/btq033.

Riera, C. E., M. O. Huising, P. Follett, M. Leblanc, J. Halloran, R. Van Andel, C. D. de Magalhaes Filho, C. Merkwirth, and A. Dillin. 2014. "TRPV1 pain receptors regulate longevity and metabolism by neuropeptide signaling." *Cell* no. 157 (5):1023-36. doi: 10.1016/j.cell.2014.03.051.

Robinson, M. D., D. J. McCarthy, and G. K. Smyth. 2010. "edgeR: a Bioconductor package for differential expression analysis of digital gene expression data." *Bioinformatics* no. 26 (1):139-40. doi: 10.1093/bioinformatics/btp616.

Sato, T., D. E. Stange, M. Ferrante, R. G. Vries, J. H. Van Es, S. Van den Brink, W. J. Van Houdt, A. Pronk, J. Van Gorp, P. D. Siersema, and H. Clevers. 2011. "Long-term expansion of epithelial organoids from human colon, adenoma, adenocarcinoma, and Barrett's epithelium." *Gastroenterology* no. 141 (5):1762-72. doi: S0016-5085(11)01108-5 [pii] 10.1053/j.gastro.2011.07.050.

bioRxiv preprint doi: https://doi.org/10.1101/118034; this version posted March 18, 2017. The copyright holder for this preprint (which was not certified by peer review) is the author/funder, who has granted bioRxiv a license to display the preprint in perpetuity. It is made available under aCC-BY 4.0 International license.

Sato, T., J. H. van Es, H. J. Snippert, D. E. Stange, R. G. Vries, M. van den Born, N. Barker, N. F. Shroyer, M. van de Wetering, and H. Clevers. 2011. "Paneth cells constitute the niche for Lgr5 stem cells in intestinal crypts." *Nature* no. 469 (7330):415-8. doi: 10.1038/nature09637 nature09637 [pii].

Saunders, C. T., W. S. Wong, S. Swamy, J. Becq, L. J. Murray, and R. K. Cheetham. 2012. "Strelka: accurate somatic small-variant calling from sequenced tumor-normal sample pairs." *Bioinformatics* no. 28 (14):1811-7. doi: 10.1093/bioinformatics/bts271.

Xue, Xiang, Sadeesh K Ramakrishnan, Kevin Weisz, Daniel Triner, Liwei Xie, Durga Attili, Asha Pant, Balázs Győrffy, Mingkun Zhan, Christin Carter-Su, Karin M Hardiman, Thomas D Wang, Michael K Dame, James Varani, Dean Brenner, Eric R Fearon, and Yatrik M Shah. "Iron Uptake via DMT1 Integrates Cell Cycle with JAK-STAT3 Signaling to Promote Colorectal Tumorigenesis." *Cell Metabolism* no. 24 (3):447-461. doi: 10.1016/j.cmet.2016.07.015.